TECHNICAL REVIEW OF THE LINED ROCK CAVERN (LRC) CONCEPT AND DESIGN METHODOLOGY: STEEL LINER RESPONSE

Prepared for:
U.S. Department of Energy
National Energy Technology Laboratory
Morgantown, West Virginia

Under:
Prime Contract No. DE-AM26-99FT40463
Subcontract No. 735937-30001-02

Prepared by:
Branko Damjanac
Carlos Carranza-Torres
Robert Dexter

Itasca Consulting Group, Inc.
Thresher Square East
708 South Third Street, Suite 310
Minneapolis, Minnesota 55415

August 2002

ref: ICG02-2062-8

EXECUTIVE SUMMARY

The storage of pressurized natural gas in large steel-lined caverns excavated in crystalline rock has been under development in Sweden for more than 10 years. Unlike the current storage technology, which relies on the existence of salt domes (or thick salt layers), aquifer formations and depleted oil fields, the lined rock cavern (LRC) concept provides the option of greater flexibility in the management of local and regional gas supplies. With the prospect of this technology being used in the commercial storage of natural gas in the United States, the U.S. Department of Energy, through the National Energy Technology Laboratory in Morgantown, West Virginia, initiated a technical review of the feasibility of the LRC storage concept and its current design methodology.

The principal idea behind the LRC gas-storage concept is to rely on a rock mass (primarily, crystalline rock) to serve as a pressure vessel in containing stored natural gas at maximum pressures from about 15 MPa to 25 MPa. The concept involves the excavation of relatively large, vertically cylindrical caverns 20 m to 50 m in diameter, 50 m to 115 m tall, with domed roofs and rounded inverts to maximize excavation stability and optimize deformation of components of cavern wall (i.e., concrete and steel liner) during the operation. The caverns are located at depths from 100 m to 200 m below the ground surface, and they are lined with approximately 1-m thick reinforced concrete and thin (12-mm to 15-mm) carbon steel liners. The purpose of the steel liner, which is the innermost liner, is strictly to act as an impermeable barrier to the natural gas. The purpose of the concrete is to provide a uniform transfer of the gas pressure to the rock mass and to distribute any local strain in the rock mass (e.g., from the opening of natural rock fractures) at the concrete/rock interface more evenly across the concrete to the steel liner/concrete interface. To further minimize local circumferential strains in the steel liner, a viscous layer ($\sim$ 5 mm thick) made of a bituminous material is placed between the steel and the concrete liners.

The LRC development has included a scaled (approximately 1:9 scale) experiment of the concept conducted at the Grängesberg Test Plant in Sweden, with reported positive results (Stille et al. 1994). A full-scale LRC demonstration facility is currently being constructed at Skallen, a site near the coastal city of Halmstad in southwest Sweden.

The LRC developments have been reflected in a current design methodology. This methodology is a probabilistic, multi-stage approach. Evaluations of the potential for a rock mass to host an LRC facility are made at different stages, with an increasing demand for geophysical information at each stage. The result is an increasingly refined design in terms of probable loads and material response. The methodology is embedded in two models: FLRC1 (Feasibility for Lined Rock Caverns 1), which is an initial procedure for LRC evaluations at an early stage; and FLRC2 (Feasibility for Lined Rock Caverns 2), a more detailed procedure for LRC evaluations and design in later stages of the development, when more site-specific geophysical information becomes available. The FLRC1

and FLRC2 models rely on rock index properties and empirical relations to estimate the rock-mass mechanical parameters (i.e., stiffness and strength); limit-equilibrium, finite-element and analytical (homogeneous and isotropic) models are used to estimate cavern location (i.e., depth), maximum gas pressure, cavern deformations, and steel-liner strain. The methodology emphasizes two key LRC design criteria associated with (a) safety against ground uplift, and (b) a maximum operating (cyclic) strain range in the steel liner.

The first phase review (Brandshaug et al. 2001) of the lined rock-cavern storage concept and design methodology focused on the feasibility of this technology and the robustness of its design methodology, primarily in the context of the mechanical response of the rock mass during cavern operation (i.e., for a pressurized cavern). The review discussed in this report is concerned mostly with the second key aspect of the LRC concept: the structural integrity and constructibility of the steel liner. Particular attention was paid to the production pipe (nozzle) and the connection between the production pipe and the cavern.

Deformation and stresses in the cavern liner for the most critical loading conditions were analyzed numerically as the part of this review. The analysis was done for different assumptions concerning the mechanical behavior of the rock mass: (a) continuous (linearly elastic and elasto-plastic), and (b) discontinuous (few discontinuities forming a single wedge or a large number of discontinuities — joints). The discreteness of the rock mass has important effect on the deformation of the cavern liner and, consequently, on the strain ranges in the the steel liner. Therefore, careful consideration of discontinuities in the rock mass should be taken during the design process. An approach based on smearing the effect of discontinuities in the rock mass may lead to non-conservative design. The predicted maximum strains and the strain range (particularly when discontinuities are present in the rock mass) are also very sensitive to the shear resistance of the bituminous layer between the steel and the concrete liner. The analysis by the LRC team of the cavern liner and the production pipe in support of design for Skallen plant is based on non-conservative assumptions that: (a) the friction angle in the bituminous layer between the steel line and the concrete is zero, and (b) the rock mass behaves as linearly elastic, continuous medium.

The analyses of the fracture and fatigue of the steel liner performed by the LRC team appear to be well substantiated and sufficiently conservative. However, some details (e.g., fillet-welded pipe foot) with large stress concentration factors were not addressed in the review documents, and the margin of safety of the steel liner to fracture is probably much less than it appears based on the analysis of the LRC team.

The technical documentation for the Skallen plant contains a comprehensive set of performance requirements for the overall design of the steel liner, required documentation, material requirements for the steel plate and filler material, erection, welding and inspection. However, the technical documentation needs to be rewritten to reference appropriate U.S. codes and to avoid duplication.

The LRC concept seems feasible from the standpoint of the structural integrity of the steel liner. However, we recommend that analysis be conducted paying more attention to details, particularly

the effects of discontinuities in the rock mass and the shear resistance of the bituminous layer between the steel liner and the concrete.

TABLE OF CONTENTS

1.0 INTRODUCTION 1

2.0 TECHNICAL REVIEW: OBJECTIVES, STANDARD AND SCOPE 1

3.0 SUMMARY OF LRC CONCEPT AND DESIGN METHODOLOGY 3

3.1 Title List of Review Documents 3

3.2 Summary of LRC Concept 4

3.3 Summary of LRC Design Methodology 4

4.0 REVIEW OF KEY LRC DESIGN ASPECTS 5

5.0 MODEL OF CAVERN AND PRODUCTION PIPE 6

5.1 Model Description 6

5.1.1 *3DEC* Model 7

5.1.2 *FLAC3D* Model 15

5.2 Deformation and Stresses in the Steel Liner 18

5.2.1 Allowable Stresses 18

5.2.2 Case 1: Continuous, Elastic Rock Mass 19

5.2.3 Case 2: Continuous, Elastic-Plastic Rock Mass 22

5.2.4 Case 4: Discontinuous Rock Mass, Wedge No. 2 25

5.2.5 Case 13: Discontinuous Rock Mass, Joints No. 13 27

5.2.6 Effect of Cyclic Loading 31

6.0 FATIGUE AND CRACK GROWTH 33

6.1 Initial Defect Size 36

6.2 Fracture Mechanics Analysis 38

6.3 Toughness Testing 39

6.4 Estimation of Toughness 40

6.5 Critical Defect Size 42

6.6 Secondary Stresses in Fracture Assessments 42

6.7 Low-Cycle Fatigue 43

6.8 Fatigue Crack Initiation Propagation 44

7.0 STANDARDS OF CONSTRUCTION 44

7.1 Design Code 45

7.2 Available Materials 46

7.3 Construction Practice and Welding Procedures 47

8.0 CONCLUSIONS 48

9.0 REFERENCES 50

LIST OF FIGURES

1 Cross-Sections Through the *3DEC* Model 8

2 Views of the Cavern in the *3DEC* Model 9

3 Cases 3 Through 10: Views of the Cavern and Considered Wedges 10

4 Cases 11 Through 13: Views of the Cavern with Joint Traces 11

5 Case1: Displacements (m) 12

6 Case 2: Displacements (m) 13

7 Case 4: Displacements (m) 13

8 Case 13: Displacements (m) 14

9 Cavern Geometry and *FLAC3D* Grid 15

10 Case 1: Displacement Vectors and Contours of Displacement Magnitude (m) in the Concrete 16

11 Case 2: Displacement Vectors and Contours of Displacement Magnitude (m) in the Concrete 16

12 Case 4: Displacement Vectors and Contours of Displacement Magnitude (m) in the Concrete 17

13 Case 13: Displacement Vectors and Contours of Displacement Magnitude (m) in the Concrete 17

14 Case 1: Forces (MN) in the Steel Liner 20

15 Case 1: Stresses (MPa) in the Production Pipe 20

16 Case 1, 5° Friction Angle Between Steel and Concrete: Forces (MN) in the Steel Liner 21

17 Case 1, 5° Friction Angle Between Steel and Concrete: Stresses (MPa) in the Production Pipe 21

18 Case 2: Forces (MN) in the Steel Liner 23

19 Case 2: Stresses (MPa) in the Production Pipe 23

20 Case 2, 5° Friction Angle Between Steel and Concrete: Stresses (MPa) in the Production Pipe 24

21 Case 4: Stresses (MPa) in the Connection Plate 25

22 Case 4: Stresses (MPa) in the Production Pipe 25

23 Case 4, 5° Friction Angle Between Steel and Concrete: Stresses (MPa) in the Connection Plate 26

24 Case 4, 5° Friction Angle Between Steel and Concrete: Stresses (MPa) in the Production Pipe 26

25 Case 13: Stresses (MPa) in the Cavern 28

26 Case 13: Stresses (MPa) in the Connection Plate 28

27 Case 13: Stresses (MPa) in the Production Pipe 29

28 Case 13, 5° Friction Angle Between Steel and Concrete: Stresses (MPa) in the Cavern 29

29 Case 13, 5° Friction Angle Between Steel and Concrete: Stresses (MPa) in the Connection Plate 30

30 Case 13, 5° Friction Angle Between Steel and Concrete: Stresses (MPa) in the Production Pipe 30

31 Case 4: Displacement Vectors and Contours of Displacement Magnitude (m) Due to First 3 Loading Cycles 32

32 Detail of Transition From the Production Pipe to the Liner 34

33 Detail of the Pipe Foot 35

34 Actual Defect Size From Destructive Examinations of Cores From Welds With UT Indications of Various dB Ratings 37

35 Fracture Toughness Data for a Number of Brittle Materials That Have Caused Fractures in the Past 41

LIST OF TABLES

1 List of Cases Analyzed with *3DEC* 10

2 Material Properties Used in the *3DEC* Model 11

3 Joint Properties Used in *3DEC* Model 12

4 Summary of Worst-Case Defects 36

1.0 INTRODUCTION

The U.S. Department of Energy (DOE), through the National Energy Technology Laboratory (NETL) in Morgantown, West Virginia, is participating in the introduction of new technology to the commercial natural-gas-storage market in the United States. For more than 10 years, Sweden has been developing a technology for storing pressurized natural gas in excavated steel-lined caverns in crystalline rock (Larsson et al. 1989; Tengborg 1989). Although existing underground space (e.g., large salt caverns, aquifer formations, depleted oil fields) is currently being used for the same purpose in the United States and abroad, the flexibility of the lined rock cavern (LRC) concept could contribute to more efficient management of the local and regional supplies of natural gas. This is particularly true for the Northeast and Northwest regions of the United States, where salt caverns and depleted oil fields do not exist. The developers of the technology expect that 50-m to 115-m tall cylindrical caverns, 20 m to 50 m in diameter, can be constructed in crystalline rock at depths of 100 m to 200 m. The caverns, which are fitted with an impermeable steel liner, are expected to provide continuous storage of natural gas for maximum gas pressures ranging from 15 MPa to 25 MPa.

A scaled (approximately 1:9) experiment of the concept has been conducted at the Grängesberg Test Plant in Sweden, with reported positive results (Stille et al. 1994). A full-scale LRC demonstration facility currently is being constructed at Skallen, a site near the coastal city of Halmstad in southwest Sweden.

With the prospect of introducing this new gas-storage technology to the United States, it is timely for DOE/NETL to assess the merits of the LRC concept and examine the details of its design methodology to ensure it is both technically feasible and safe. The rock mechanics aspects of the LRC concept and design methodology were the subject of a separate technical review (Brandshaug et al. 2001) available at DOE's NETL Web site www.netl.doe.gov. The following is a technical review that focuses primarily on the steel liner/nozzle structural integrity and constructability.

2.0 TECHNICAL REVIEW: OBJECTIVES, STANDARD AND SCOPE

An earlier DOE-sponsored LRC project (U.S. Department of Energy 2000) addressed the current state-of-the-art in the LRC concept, market data for conventional alternative storage in the Northeastern United States, identification and selection of two generic geologic sites, conceptual design for the LRC, cost estimate, economic comparison of LRC to alternatives, and environmental impact and permitting issues. The currently sponsored project complements the previous work by adding an independent review of the LRC storage technology. The specific objective of the current review was to evaluate steel liner/nozzle structural integrity and constructability.

An independent technical review was initiated with a meeting between the LRC development group, NETL and Itasca Consulting Group Inc. (the review team) in September 2000. At that time, the LRC group consisted of Energy East Enterprises, Inc. (USA), Gas de France International, S.A., Sydkraft

AB (Sweden), and Enron North America Corporation. At this meeting, several presentations were made by the LRC group with regard to the technical aspects of the lined rock cavern concept and its design methodology. Key aspects of the LRC design were identified (e.g., safety against ground uplift and maximum steel-liner strain range), and results from a pilot study in Grängesberg, Sweden, were presented.

It was clear that in addressing the specific review objective, two important components of mechanics are involved:

1. Rock Mechanics (because a stable rock mass is imperative to the success of the concept during both the cavern-excavation and storage-operation periods); and

2. Structural Mechanics (because the structural integrity of the steel-liner and nozzle (production pipe) assembly is crucial to the continuous service of the liner as an impermeable barrier to the stored natural gas).

Subsequent to the September meeting, the review team received a number of review documents from the LRC group. These documents (some of which contain confidential information) provide in-depth technical details of the LRC concept, the design methodology, and test results of the pilot study. The first phase of the technical review, which concerned rock mechanics issues, was based on the information in the review documents and on the initial technical presentations made by the LRC group at the September 2000 meeting. After completion of the first phase of the review, the technical review team proceeded to evaluate the second key issue regarding the LRC concept. The second phase of the review is based on reports and documentation provided for the first phase and additional documentation provided to the review team by the LRC group during the second part of 2001. The complete list of technical documentation used in the review is given in Section 3.1. The review discussed in this report is concerned with the structural mechanics aspect of the LRC concept only — specifically, issues related to the steel liner (e.g., evaluation of liner fatigue).

While an independent complete LRC design analysis was not performed as part of this review, some analyses were conducted that evaluated key design criteria associated with the rock mass and the steel-liner response for LRC conditions. The results of these analyses generally agreed with results expressed in the review documents. The results show important effects from the presence of natural rock fractures on local strains in the steel liner during cavern pressurization. Such effects are not accounted for in the current LRC design methodology, because it regards the rock mass only as a continuum. When a rock mass is represented as a continuum, the deformational effects of natural rock fractures are smeared/averaged throughout the rock mass. Although this is frequently done in rock engineering, the importance of the steel-liner strain in the context of the LRC design also warrants evaluation using methods that account for local effects associated with the presence of explicit rock fractures.

3.0 SUMMARY OF LRC CONCEPT AND DESIGN METHODOLOGY

For completeness of documentation, the LRC concept and design methodologies are briefly summarized. This summary is constructed from the review documents supplied by the LRC group. A title list identifying these documents is provided below.

3.1 Title List of Review Documents

The following is a list of the review documents, provided to the review team by the LRC group, which are used as a basis for review of the structural mechanics aspects of the LRC concept.

1. Report (confidential) "Cavern Wall - Demo Plant Design", June 2000;
2. Etude d'integrite d'un defaut dans un revetement (or, in English, Study of the Effect of a Defect on the Integrity of a Liner), Framatome, May 2000;
3. Defect Assessment of the LRC Demo Plant Lining, Det Norske Veritas, Report No. 10172300-1, Revision No. 1 May 2000;
4. Defect Assessment of the LRC Demo Plant Lining, Det Norske Veritas, Report No. 10460200-1, Revision No. 2, April 2001;
5. Report (confidential) "Underground Gas Storage — Static Analysis for the Liner, Connection Plate and Production Pipe", Ref.: K98_1101, Gaz de France, November 2001;
6. LRC Natural Gas Storage Project — Lining Works, STEEL LINING, Document 11.2;
7. Report (confidential), "LRC Demo Plant, Global Rock Mass Parameters for the Skallen Site";
8. Report (confidential), "Rock Mechanics Criteria for Location of a LRC Storage".
9. Design drawings for the Skallen plant by Skandinavisk Industriservice A/S, provided to Itasca Consulting Group by Ola Hall of Sycon Energikonsult;
   (a) Pipe Foot, Drawing No. 669-021 Rev. C
   (b) Culvert – General Arrangement, Drawing No. 669-023 Rev. A
   (c) Shaft Piping at Cavern Top – General Arrangement, Drawing No. 669-024 Rev. C
   (d) Instrumentation Inside Cavern – General Arrangement, Drawing No. 660-025 Rev. B
   (e) Shaft Tunnel – General Arrangement, Drawing No. 669-026 Rev. A
   (f) Connection Plate, Drawing No. 669-033 Rev. A

3.2 Summary of LRC Concept

The principal idea behind the LRC gas-storage concept is to rely on a rock mass (primarily crystalline rock) to serve as a pressure vessel in containing stored natural gas at maximum pressures from about 15 MPa to 25 MPa. The concept involves the use of relatively large, vertically cylindrical caverns 20 m to 50 m in diameter, 50 m to 115 m tall, with domed roofs and rounded inverts to maximize excavation stability. The caverns are located at depths from 100 m to 200 m below the ground surface, and they are lined with approximately 1-m thick reinforced concrete and thin (12-mm to 15-mm) carbon steel liners. The purpose of the steel liner, which is the innermost liner, is strictly to act as an impermeable barrier to the natural gas. The purpose of the concrete is to provide a uniform transfer of the gas pressure to the rock mass and to distribute any local strain in the rock mass (e.g., from the opening of natural rock fractures) at the concrete/rock interface more evenly across the concrete to the steel liner/concrete interface. To further minimize local circumferential strains in the steel liner, a viscous layer ($\sim$ 5 mm thick) made of a bituminous material is placed between the steel and the concrete liners.

Pressurization of the gas increases the gas density (i.e., mass per unit volume) and is key to making the storage concept economically viable. An operating cavern is expected to go through pressure cycles from approximately 3 MPa to 25 MPa during periods of gas depletion and recharge, as demand dictates, and may have a nominal design life of 500 cycles. For circumstances in which groundwater is present, the gas pressure also provides structural support to the relatively thin steel liner, which is not designed to withstand external water pressure.

It is expected that the LRC concept can be applied to a variety of different rock types and to rocks of varying strengths and deformabilities.

3.3 Summary of LRC Design Methodology

The review documents present the LRC design methodology as a stochastic, multi-stage development approach. Evaluations of the potential for a rock mass to host an LRC facility are made at different stages, with an increasing demand for geophysical information in each stage. The result is an increasingly refined design in terms of probable loads and material response. The methodology is embedded in two models: FLRC1 (Feasibility for Lined Rock Caverns 1), which is an initial procedure for LRC evaluations at an early stage; and FLRC2 (Feasibility for Lined Rock Caverns 2), a more detailed procedure for LRC evaluations and design in later stages of the development, when more site-specific geophysical information is available.

Development includes the following stages.

1. Initial exploration uses limited, generally available geological information (e.g., from surface observations and any previous underground work in the area) as the basis for estimating rock mass quality, which, in turn, is used in the initial model (FLRC1) to assess the potential for the rock mass to host an LRC facility.

2. Increasingly detailed site characterization is aimed specifically at determining the best underground location for the LRC. Details of the rock mass are obtained from core logs and other geophysical investigations. Rock index properties are determined from rock cores, and a "better" estimate (in terms of confidence) of rock mass quality is made. Estimates of maximum gas pressure and liner strains are made stochastically, using the procedure in the FLRC2 model. These estimates are used as the basis for the initial LRC design.

3. During the construction stage, additional site characterization is conducted, and the Observational Approach is used to provide the "best" estimates of likely cavern response. The new estimates in this phase may affect the final LRC design.

The FLRC1 and FLRC2 models rely on rock index properties and empirical relations to estimate the rock mass mechanical parameters (i.e., stiffness and strength); limit-equilibrium, finite-element and analytical (homogeneous and isotropic) models are used to estimate cavern location (i.e., depth), maximum gas pressure, cavern deformations, and steel liner strain. The methodology emphasizes two key LRC design criteria associated with (1) safety against ground uplift, and (2) a maximum operating (cyclic) strain range in the steel liner.

4.0 REVIEW OF KEY LRC DESIGN ASPECTS

According to the review documents, LRCs are expected to operate at maximum gas pressures of 15 MPa to 25 MPa. With the caverns located at a relative shallow depth of 100 m to 200 m, this generally means the rock mass could be subjected to pressures 4 to 8 times higher than the in-situ rock-mass stresses. Because the LRC concept relies on the rock (not the steel or concrete liners) to serve as the pressure vessel, an adequate cavern depth (or rock overburden) is important. The overburden rock mass must resist the maximum cavern pressure in a stable manner. This key aspect of the LRC design was evaluated in the first phase of the review (Brandshaug et al. 2001).

For a given cavern geometry, the mechanical response of the cavern wall to the LRC pressure depends on the site-specific character of the rock mass and on the structural interaction between the rock mass, concrete liner, viscous bituminous layer, and the steel liner. In general, the gas pressure will displace the cavern wall radially outward, resulting in extensional strains in the tangential horizontal and vertical directions in the steel liner, concrete liner, and in the rock at the cavern wall. For a given pressure, the amount of extensional strain depends mostly on the rock mass strength and deformability, which become important attributes of the LRC design. The cavern wall response and its affect on the steel liner strain are evaluated in this section.

Note that the parts of this review requiring evaluation using numerical models have considered conditions at the Skallen demonstration plant, which is currently being constructed near the coastal city of Halmstad in southwest Sweden.

5.0 MODEL OF CAVERN AND PRODUCTION PIPE

The cavern wall and the steel liner were subjects of the first phase of the review (Brandshaug et al. 2001). However, the conducted analyses of stresses and deformation (strain) in the different components of the cavern wall were simplified, assuming either plane strain or axisymmetric conditions of deformation. A three-dimensional analysis of the cavern and surrounding rock mass has been conducted as a part of the review discussed in this report. The objective was to investigate the effect of anisotropy and localized deformations of the rock mass on stresses and deformation in the concrete and steel liners, particularly in the production pipe (nozzle) and the connection plate.

5.1 Model Description

The three-dimensional deformation and stresses in the liner of an LRC cavern and the interaction between the cavern and the surrounding rock mass were simulated using two codes: *3DEC* (Itasca Consulting Group, Inc. 1998) and *FLAC3D* (Itasca Consulting Group, Inc. 2002). *3DEC* is a code well-suited to analyze the deformation of a discontinuous rock mass. It represents the rock mass as an assembly of polyhedral deformable blocks in three-dimensional space that can interact mechanically along the contacts — discontinuities in the rock mass (i.e., joints). The interfaces between blocks in *3DEC* follow an elastic-plastic stress-displacement relation. The condition for a relative slip of blocks along an interface is governed by a Coulomb law. If the tensile strength of the contact, which is usually zero, is overcome, the blocks separate, creating a gap between them. The contacts between blocks are created and lost automatically as a result of their displacements. Unfortunately, *3DEC* does not have very robust logic for representing the mechanical behavior of thin structures that behave as shells (e.g., steel liner). A more detailed description of *3DEC* and its formulation can be found in the *3DEC* User's Manual.

FLAC3D is a three-dimensional numerical code for simulating the deformation of continuous media. A number of constitutive models are available to represent the mechanical behavior of solids. *FLAC3D* also has a built-in logic for representation of different types of structural elements, including shell/liner structural elements. These elements are well-suited for representation of deformation and stresses in the steel liner. The shell structural elements, similar to other structural elements in *FLAC3D*, can interact with the surrounding medium, which is represented by three-dimensional solid elements. The interaction is simulated by the linearly elastic-plastic contact with a slip condition expressed by the Coulomb law. If tensile stress across the contact overcomes the tensile strength, the shell/liner detaches from the solid grid, and a gap appears. *FLAC3D* can handle small numbers of discontinuities in the solid model, but it is not well-suited for simulating problems for which it is essential to include a large number of discontinuities.

Considering the advantages and limitations of *3DEC* and *FLAC3D*, the analysis was conducted by coupling models, with the *3DEC* model primarily being responsible for predicting the rock mass response, and the *FLAC3D* model being responsible for predicting the liner and the nozzle response. The common boundary (i.e., coupling boundary) shared by the two models was the outside surface

of the concrete liner. The coupling between two models was one-directional: the displacements calculated by the *3DEC* model were transferred as boundary conditions to the *FLAC3D* model; no information was transferred back from the *FLAC3D* model to the *3DEC* model. The reason for one-directional coupling was the fact that the *3DEC* model included both the rock mass and the liner, while the *FLAC3D* model included the liner only. Thus, the analysis was conducted in two steps.

1. Detailed deformation of the rock mass was calculated using the *3DEC* model, which included a concrete lining in the cavern and in the production pipe. The steel liner was represented in a simplified manner inside the production pipe only. The steel liner was ignored inside the cavern because it has very little effect on the deformation of the surrounding rock mass. The predicted displacements of the outside surface of the concrete liner were transferred as boundary conditions to the *FLAC3D* model.

2. Detailed stresses and deformation of the cavern steel and concrete liners were analyzed using the *FLAC3D* model. This model also included an effect of the bituminous layer between these liners in the form of a sliding interface. The concrete liner was represented using solid zones (5 zones across the liner thickness), while the steel liner was represented using the *FLAC3D* shell structural elements. As a result of the initial and boundary conditions (i.e., inside cavern gas pressure and the external concrete liner displacements from the *3DEC* model), the *FLAC3D* model calculated stresses and displacements in the steel and concrete liners.

5.1.1 3DEC Model

The geometry of the *3DEC* model in horizontal and vertical cross-sections, with indicated initial and boundary conditions, is shown in Figure 1. The cavern is 53 m high, with a 36-m diameter. The top of the cavern is located 107 m below the ground surface. The model extends one cavern size below and above the cavern and two cavern diameters laterally from the cavern wall. “Roller” boundary conditions were used on the bottom and the vertical model boundaries. A stress boundary condition equal to the dead weight of the overburden was applied to the top model boundary. Vertical stress was assumed to be gravitational. One horizontal principal stress is equal to the vertical stress; the other is twice the vertical stress. The geometry of the cavern in the *3DEC* model is shown in two isometric views (side and top) in Figure 2. The concrete liner is represented explicitly in the *3DEC* model. The steel liner inside the cavern is neglected. Simple calculation shows that stiffness of the 15-mm thick steel liner inside the cavern is negligible compared to the stiffness of the rock mass and the concrete liner. However, the stiffness of the steel liner inside the production pipe becomes a significant part of the overall stiffness and is taken into account. The steel liner inside the production pipe was not represented explicitly in the *3DEC* model. Instead, the gas pressure acting inside the production pipe was corrected based on the deformation of the pipe’s inside wall [An analytical solution (Timoshenko and Goodier 1970) for a pressurized circular ring was used.], accounting for the force taken by the steel liner. This approximation was used in the *3DEC* model in calculating

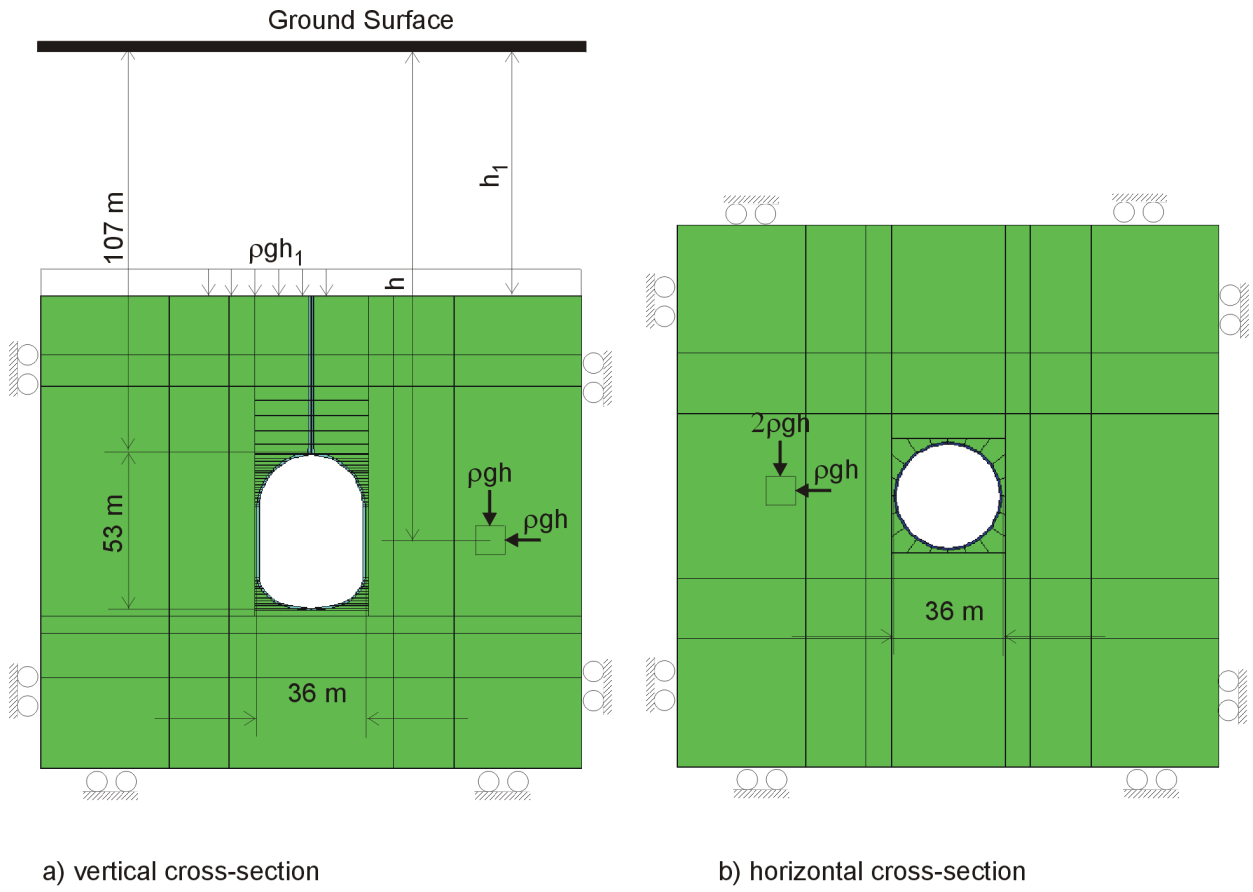

Note: Lines appearing in the figure are construction lines used during creation of the model. They do not represent discontinuities in the model, nor do they effect its response.

Figure 1 Cross-Sections Through the 3DEC Model

the rock mass deformation. The *FLAC3D* model, which is used to analyze the deformation and stresses in the cavern wall (concrete and steel liners), represents the steel liner explicitly.

The cavern undergoes different loading conditions (mainly due to the filling and emptying of the gas from the cavern) during its operation. For design purposes, the different loading conditions need to be investigated in order to determine those that are critical with respect to stability and operation of different parts of the structure. The analysis presented here was done for one loading case only, that which, among the cases declared as "required" in Review Document 5, results in the maximum stresses in the steel liner. (Some of the cases declared as "extended" cases in Review Document 5 result in larger stresses in the steel liner than Case 2 considered here. However, "extended" cases were characterized as "not necessarily realistic" and, therefore, not considered in the analysis presented in this report.) Loading Case 2 from Review Document 5 includes an isotropic gas pressure of 23 MPa inside the cavern and the production pipe, a concrete temperature

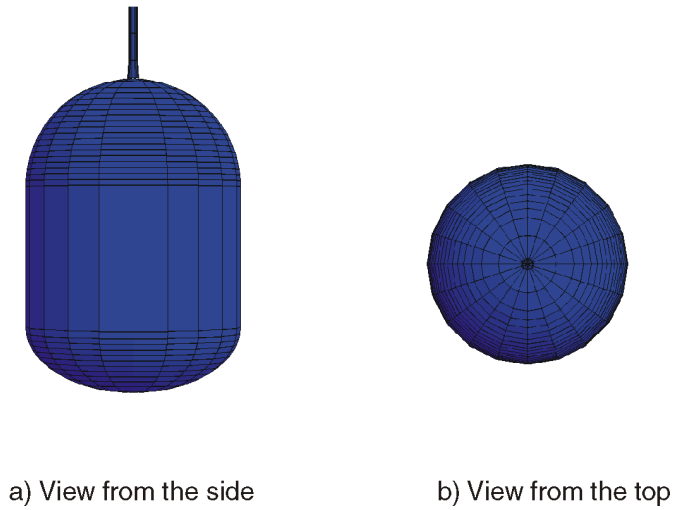

Figure 2 Views of the Cavern in the 3DEC Model

of 15° C, and a steel temperature of 30° C. Vertical push of the gas at the well head is neglected in this analysis. Even very small shear resistance between the steel liner and the concrete liner will transfer the resulting force from the steel into the concrete and the rock mass over a 100-m length of the production pipe. As a result of this assumption, the cases for assumed zero shear resistance between the steel and the concrete show some compressive vertical stresses in the production pipe. Those stresses are small and inconsequential. Therefore, the assumption is valid and conservative.

The analysis was done assuming different material behaviors for the rock mass and the concrete. The list of all cases considered is shown in Table 1. The base case (Case 1) is for the condition of linearly elastic behavior for the rock mass and the concrete, which are assumed to behave as continua. Case 2 assumes elastic-plastic constitutive behavior for the rock mass and the concrete, also assumed to be continuous. The LRC team analyzed the cavern wall using the same assumptions about rock mass behavior as those used in Cases 1 and 2.

One objective of the analyses presented in this report was to first establish agreement of results for Cases 1 and 2 with corresponding LRC results. Subsequent analysis of the cases in which the rock mass was modeled as a discontinuum (behavior not investigated by LRC team) was supposed to demonstrate the significance and the consequences of the continuum assumption. A number of different conditions were considered in the discontinuum analyses. The effect of a single wedge was considered in Cases 3 through 10. Wedges of different sizes and locations around the cavern were assumed and analyzed. All wedge cases are listed in Table 1. Figure 3 shows the geometry of the cavern and the considered wedges of the rock mass. The figure also shows the joint (joints that create the wedges) traces on the concrete wall. (The traces outline the differently colored regions on the concrete surface in Figure 3.)

Table 1 List of Cases Analyzed with 3DEC

Case	Model Description
1	continuous, elastic rock mass
2	continuous, elastic-plastic rock mass
3	discontinuous rock mass, wedge No. 1
4	discontinuous rock mass, wedge No. 2
5	discontinuous rock mass, wedge No. 3
6	discontinuous rock mass, wedge No. 4
7	discontinuous rock mass, wedge No. 5
8	discontinuous rock mass, wedge No. 6
9	discontinuous rock mass, wedge No. 7
10	discontinuous rock mass, wedge No. 8
11	discontinuous rock mass, joints No. 1
12	discontinuous rock mass, joints No. 2
13	discontinuous rock mass, joints No. 3

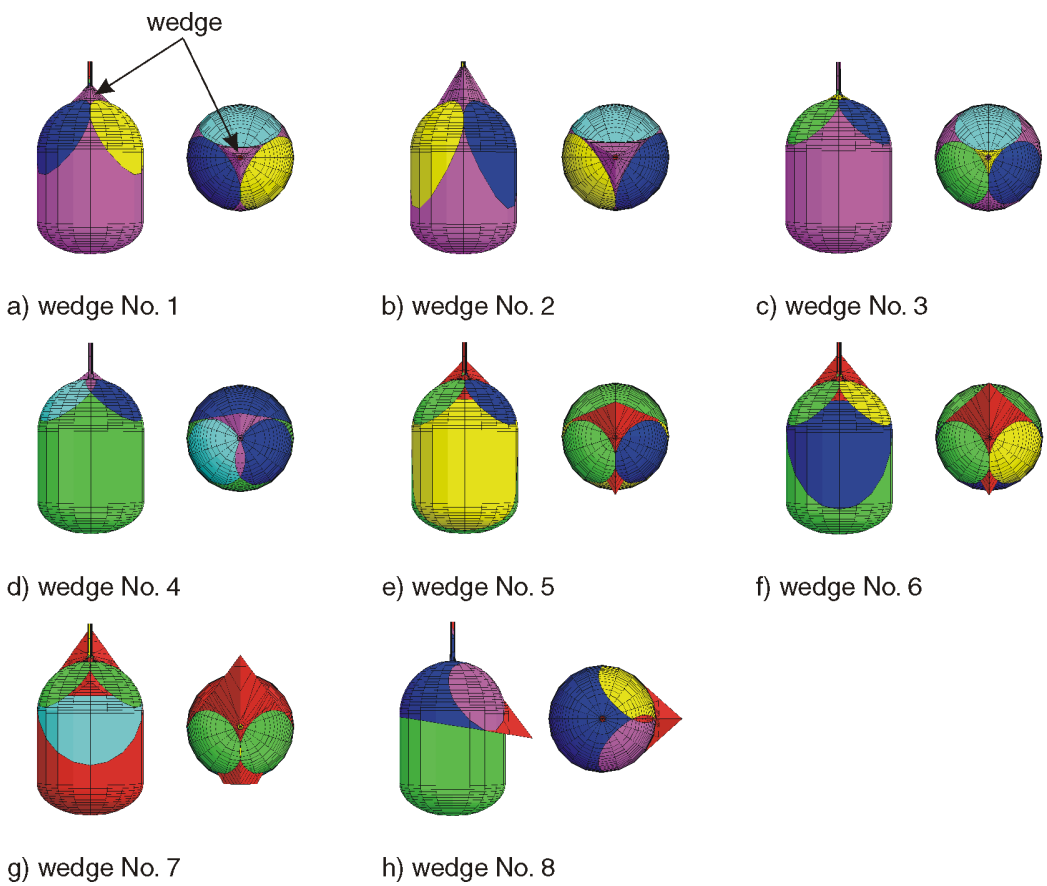

Figure 3 Cases 3 Through 10: Views of the Cavern and Considered Wedges

A large number of joints were represented explicitly in Cases 11 through 13 (Table 1). Three mutually orthogonal joint sets with joint spacings of 5 m and 8 m were assumed in Cases 11 and 13 respectively. Four joint sets at 7-m spacing were assumed in Case 12. Joint traces on the concrete liner for 3 cases are shown in Figure 4.

a) joints No. 1 b) joints No. 2 c) joints No. 3

Figure 4 Cases 11 Through 13: Views of the Cavern with Joint Traces

All cases of rock wedges and jointing discussed here were selected arbitrarily. They do not represent actual conditions at the Skallen plant or at any other potential LRC site. The objective of the analysis was to demonstrate the effect of discreteness of the rock mass on behavior of the cavern wall. Also, the effects of size, shape and position of the wedges are investigated.

The mechanical properties of the rock mass and the concrete used in the analysis are listed in Table 2. Properties correspond to conditions existing at the Skalen plant according to Review Document 1. The mechanical joint properties used in the analysis, listed in Table 3, are selected as typical joint properties. They are not based on testing or measurements at the Skallen plant.

Table 2 Material Properties Used in the 3DEC Model

Parameter	Rock Mass	Concrete
Bulk Modulus (GPa)	20	16.7
Shear Modulus (GPa)	15	12.5
Friction Angle (°)	34	45
Dilation Angle (°)	0	0
Cohesion (MPa)	13.4	9.6
Tensile Strength (MPa)	0	2.7
Density (kg/m^3)	2400	2400

Table 3 Joint Properties Used in 3DEC Model

Parameter	Value
Normal Stiffness (GPa)	10
Shear Stiffness (GPa)	10
Friction Angle (°)	30
Dilation Angle (°)	0
Cohesion (MPa)	0
Tensile Strength (MPa)	0

Displacements in cross-sections calculated in the *3DEC* model are shown for Cases 1 (continuous, elastic rock mass), 2 (continuous elastic-plastic rock mass), 4 (wedge No. 2) and 13 (joints No. 3) in Figures 5 through 8. These cases are selected for presentation, as their results were the most typical. The maximum displacement of the cavern wall for Cases 1 and 2 (continuous, elastic and elastic-plastic behavior of the rock mass) is in a good agreement with results obtained using the plane strain and the axisymmetric approximation reported in Review Document 1, as well as in Itasca's report on the first phase review of the LRC concept (Brandshaug et al. 2001). The maximum radial displacement in the middle of the cavern is 0.0115 m and 0.013 m for Cases 1 and 2, respectively (Figs. 5 and 6).

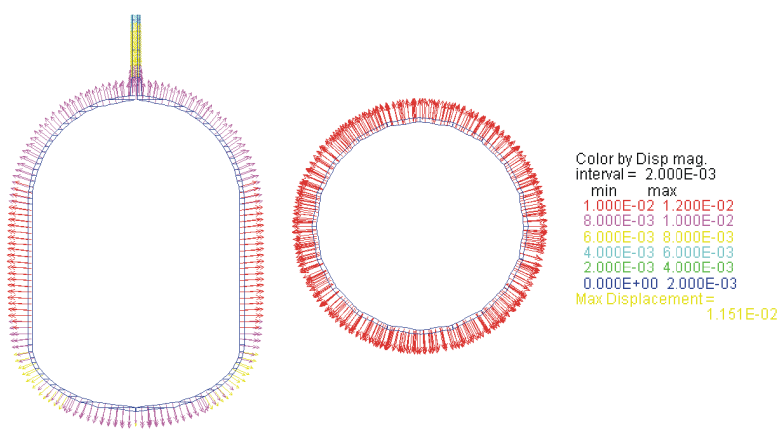

a) vertical section b) horizontal section

Figure 5 Case1: Displacements (m)

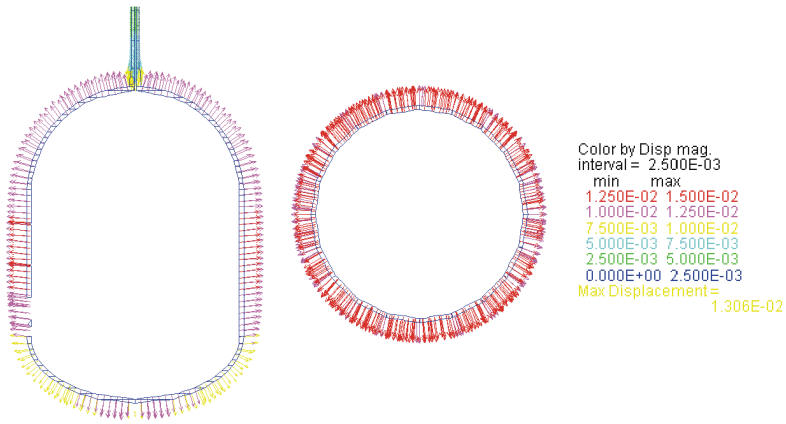

a) vertical section b) horizontal section

Figure 6 Case 2: Displacements (m)

Figures 7 and 8 show displacements for Cases 4 and 13, which assume a discontinuous rock mass. The maximum displacements do not occur necessarily in the middle of the cavern. Instead, the location of the maximum displacement is controlled by the locations where the discontinuities intersect the cavern. The maximum displacements are significantly larger than those predicted by the continuous models (i.e., 0.024 m for Case 4, and 0.044 m for Case 13). However, large gradients of displacements resulting in strain concentrations (virtually a discontinuous displacement field, compared to the smooth displacement field in the case of assumed continuous rock-mass behavior) appear to be the most significant effects influencing performance of the cavern wall and, particularly, the steel liner. Discontinuities in the displacement field are quite obvious in Figures 7 and 8.

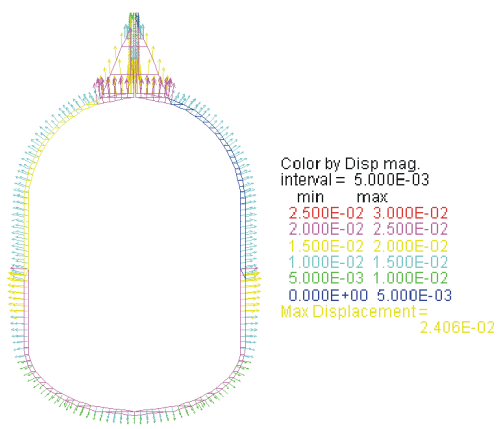

Figure 7 Case 4: Displacements (m)

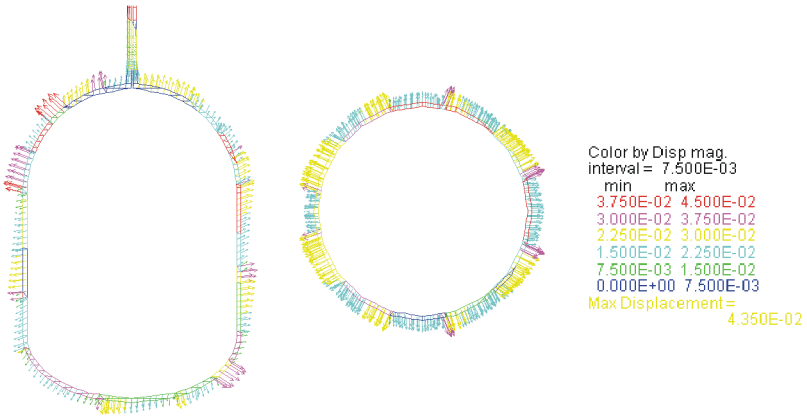

a) vertical section b) horizontal section

Figure 8 Case 13: Displacements (m)

5.1.2 FLAC3D Model

Geometry of the *FLAC3D* model is shown in Figure 9. The model includes the cavern wall (composed of the concrete and the steel liners) only. During the simulation, the outside surface of the concrete liner is moved according to displacements calculated in *3DEC* for the considered loading case and assumed behavior of the rock mass. The concrete liner is represented by five solid zones (elements). The concrete zones behave as an elastic-plastic Mohr-Coulomb material. The steel liner was represented with two-dimensional shell-type structural elements, which can carry both membrane and bending forces. The steel liner in the *FLAC3D* model behaves as a linearly elastic material. The elastic constants of steel were assumed to be: Young's modulus, $E = 210$ GPa; and Poisson's ratio, $\nu = 0.3$. An interface element simulates the behavior of the low-friction bituminous layer between the concrete and the steel liner. Two conditions of friction in the bituminous layer were analyzed: an upper bound case, with a friction angle of 5°; and a lower bound case with a 0° friction angle.

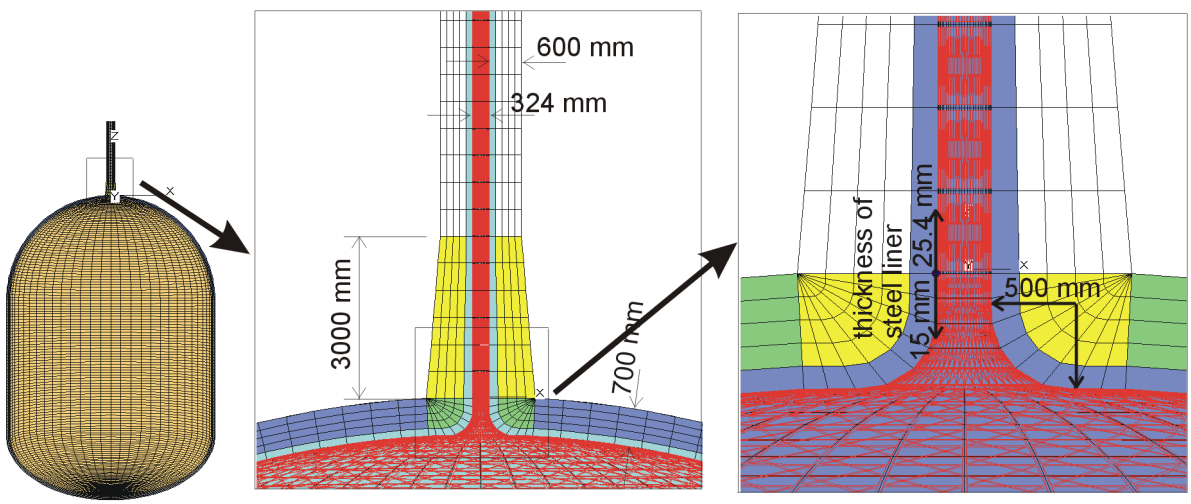

Figure 9 Cavern Geometry and FLAC3D Grid

Predicted displacements after application of 23-MPa gas pressure inside the cavern for Cases 1, 2, 4 and 13 are shown in Figures 10 through 13, respectively. The figures show displacement vectors in the vertical cross-section and contours of displacement magnitudes on the visible cavern surface behind the cross-section plane. Two views of the cavern are shown in each figure: one of the entire cavern, with a part of the production pipe; and the other of a detail of the connection between the production pipe and the cavern. Comparison of Figures 10 through 13 with the *3DEC* results shown in Figures 5 through 8 confirms that the displacement fields were transferred correctly from the *3DEC* model to the *FLAC3D* model.

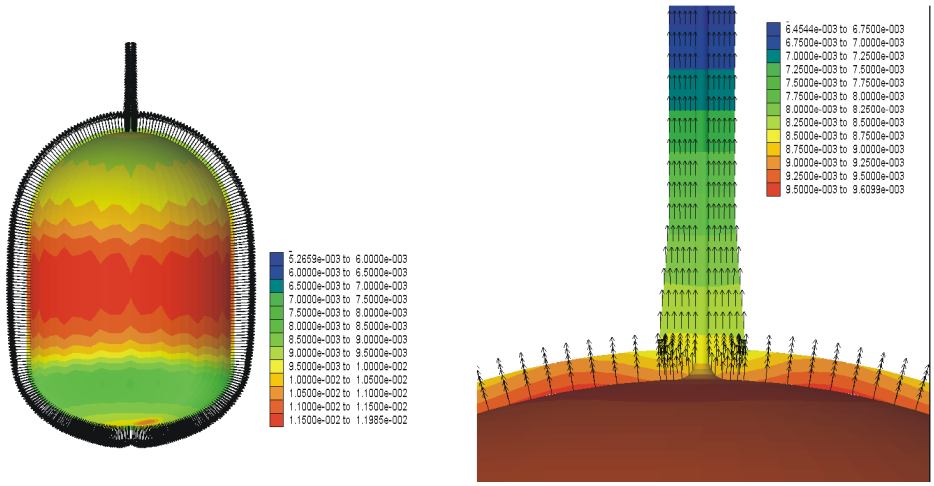

a) vertical section

b) vertical section - detail of connection between the production pipe and the cavern

Figure 10 ***Case 1: Displacement Vectors and Contours of Displacement Magnitude (m) in the Concrete***

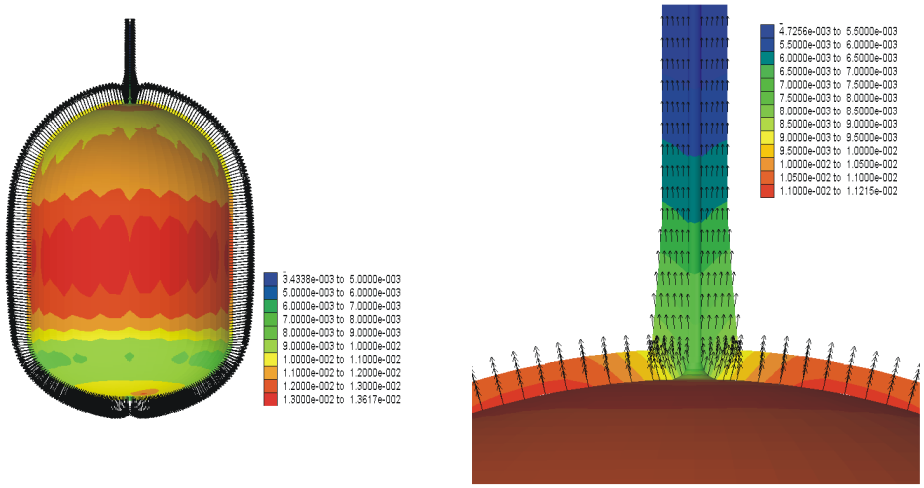

a) vertical section

b) vertical section - detail of connection between the production pipe and the cavern

Figure 11 ***Case 2: Displacement Vectors and Contours of Displacement Magnitude (m) in the Concrete***

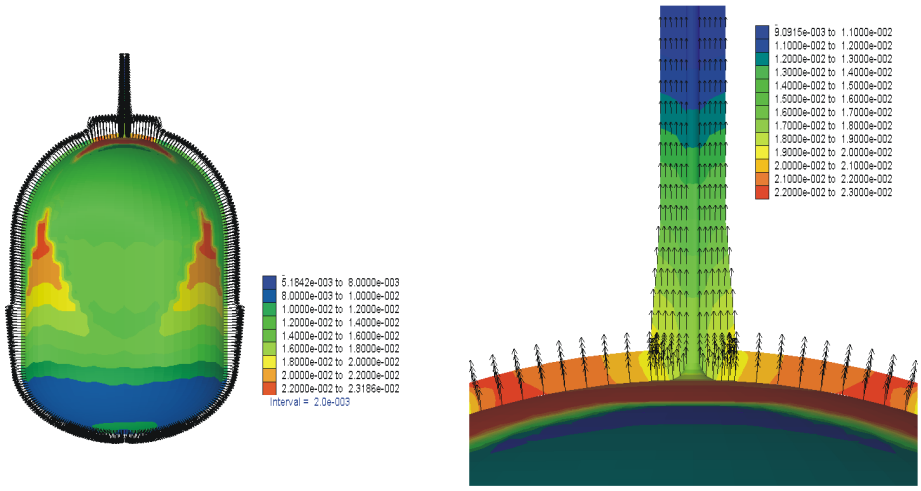

a) vertical section

b) vertical section - detail of connection between the production pipe and the cavern

Figure 12 ***Case 4: Displacement Vectors and Contours of Displacement Magnitude (m) in the Concrete***

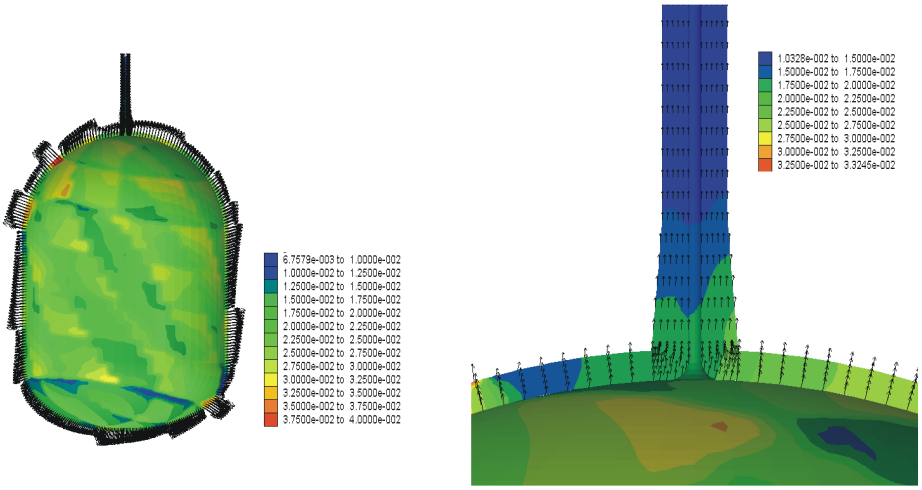

a) vertical section

b) vertical section - detail of connection between the production pipe and the cavern

Figure 13 ***Case 13: Displacement Vectors and Contours of Displacement Magnitude (m) in the Concrete***

5.2 Deformation and Stresses in the Steel Liner

5.2.1 Allowable Stresses

Analysis of stresses in the production pipe and connection plate was conducted by the LRC group, as presented in Review Document 5, according to CODAP (the French pressure vessels/exchangers code). The stress levels are assessed using the Tresca criterion:

$$\sigma_{\mathrm{t}} = \sigma_1 - \sigma_3 \leq \sigma_{\mathrm{a}} \tag{1}$$

where σ_{t} = the Tresca stress,
σ_1 = the major principal stress,
σ_3 = the minor principal stress,
σ_{a} = $k\sigma_y/1.6$, allowable Tresca stress,
σ_y = the yield stress of the steel, and
k = the coefficient specified in CODAP according to the loading type.

For the steel liner in the cavern and the production pipe, a k-coefficient equal to 3 (for the conditions of displacement-controlled loading) is recommended by CODAP. The analysis in Review Document 5 was done assuming a steel yield stress, σ_y, equal to 267 MPa. Consequently, the allowable Tresca stress, σ_{a}, is 500.6 MPa. However, in other review documents (e.g., Review Document 1), the yield stress of steel was assumed to be 355 MPa, which suggests that the allowable Tresca stress should be 665 MPa.

The stress analysis proposed by the ASME Boiler and Pressure Vessel Code (1998a), Section VII – Division 2, Appendix 4, "Mandatory Design Based on Stress Analysis" uses "Stress Intensities", S (not to be confused with the fracture mechanics parameter, K), the same as σ_{t} defined in Equation 1.

The tabulated allowable stress, S_m, is 1/3 of the uniaxial ultimate tensile strength. S from the primary membrane stress must be less than S_m. S from local and bending stresses must be less than $1.5S_m$ (i.e., equal to 50% of ultimate tensile strength). S from the local and bending stresses plus secondary stresses must be less than $3S_m$ (i.e., equal to ultimate tensile strength).

In the ASME code, the stress due to internal pressure in the steel liner should be considered a secondary stress. The definition of primary stress is:

> *"A normal stress or a shear stress developed by the imposed loading which is necessary to satisfy the simple laws of equilibrium of external and internal forces and moments. The basic characteristic of a primary stress is that it is not self-limiting. Primary stresses which considerably exceed the yield strength will result in failure or at least in gross distortion."*

On the other hand, the definition of secondary stress is:

> *"A normal stress or a shear stress developed by the constraint of adjacent parts or by self-constraint of a structure. The basic characteristic of a secondary stress is that it is self-limiting. Local yielding and minor distortion can satisfy the conditions which cause the stress to occur and failure from one application of the load is not to be expected."*

In the case of the LRC, the steel liner just contains the gas (prevents it from leaking), while the load is carried mostly by the surrounding rock mass. Therefore, the stress is "self-limiting" according to ASME and would be considered secondary stress. Therefore, S from all stresses must be less than the ultimate tensile strength of the steel, or 490 MPa. This is much less than the allowable stress under CODAP. The steel liner is under displacement-controlled loading — in which case, strains, fracture and fatigue are better measures of the limiting condition in the steel liner. Fracture and fatigue are discussed in more detail in Section 6.0. Provisions of CODAP with regard to allowable stresses seem to be more reasonable than ASME Boiler and Pressure Vessel Code for the LRC-type of structure.

Note that all the calculations presented here are based on the assumption of linearly elastic behavior for the steel liner. Consequently, because the stress–strain curve for steel is highly non-linear for stress levels larger than the yield stress, calculated stresses larger than the yield stress (and particularly larger than the ultimate tensile stress) are not correct representations of stress levels in the liner.

5.2.2 Case 1: Continuous, Elastic Rock Mass

The membrane forces in the steel liner for Case 1 (which assumes continuous, linearly elastic behavior of the rock mass, and negligible shear resistance in the interface between the concrete and the steel) are shown in Figure 14. (The tangential vertical and horizontal stresses can be obtained from the membrane forces by dividing them by the thickness of the steel liner.) The maximum horizontal stress is approximately 135 MPa; the maximum vertical stress is 90 MPa. The maximum strain of 0.05% in the horizontal direction in the middle of the cavern clearly indicates conditions corresponding to high-cycle fatigue. The major and minor principal stresses in the production pipe (shown in Fig. 15) are within acceptable limits: the Tresca stress is approximately 200 MPa, which is less than the allowable stress. The forces and stresses in the steel liner and the production pipe for the same conditions — but assuming a 5° friction angle in the bituminous layer — are shown in Figures 16 and 17. The maximum vertical stress is 180 MPa at the transition between the vertical wall and the invert. The corresponding strain is 0.07%. The horizontal stress in the middle of the height of the cavern is 115 MPa. The corresponding strain is 0.055%. These stress and strain levels are within the limits for high-cycle fatigue. However, the plot of principal stresses in the production pipe (Fig. 17) shows that the compressive (vertical) stress at the transition between the steel liner thickness of 15 mm and 25.4 mm is of the order of 450 MPa. The high compressive stresses are generated as a result of a vertical push of the production pipe by the cavern wall, and the

shear resistance in the interface between the steel and the concrete, to the vertical movement of the production pipe. Such high stresses in the steel indicate potential buckling problems and warrant detailed analysis. The maximum Tresca stress, a difference between the major and minor principal stresses, is 550 MPa, larger than the allowable stress of 500.6 MPa, but less than the 665-MPa allowable stress for steel with a yield stress of 355 MPa (according to the French CODAP code). Note that this Tresca stress exceeds the 490-MPa limit that would be allowable under the ASME code.

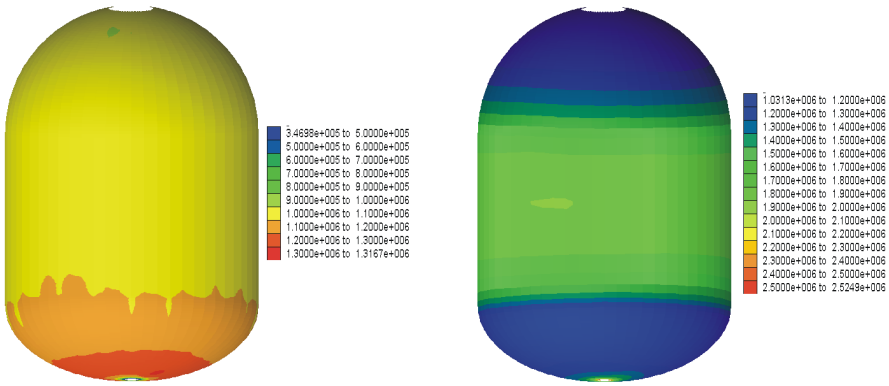

a) vertical force b) horizontal force

Note: To obtain the stress, the force should be divided by steel liner thickness (i.e., 15 mm)

Figure 14 Case 1: Forces (MN) in the Steel Liner

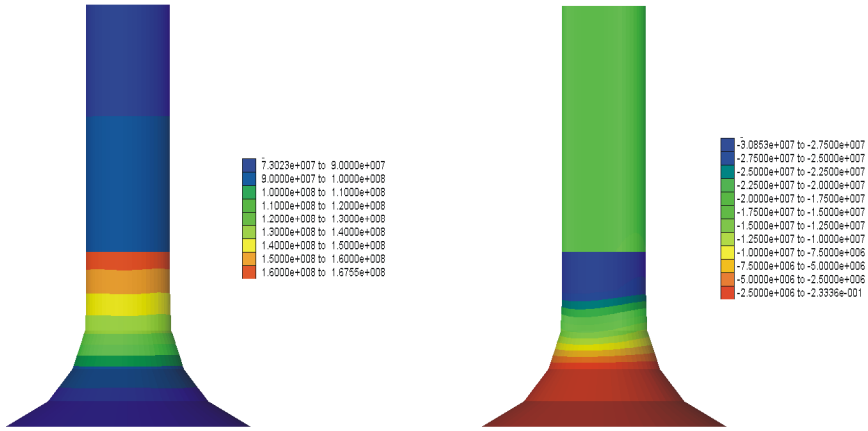

a) major principal stress b) minor principal stress

Figure 15 Case 1: Stresses (MPa) in the Production Pipe

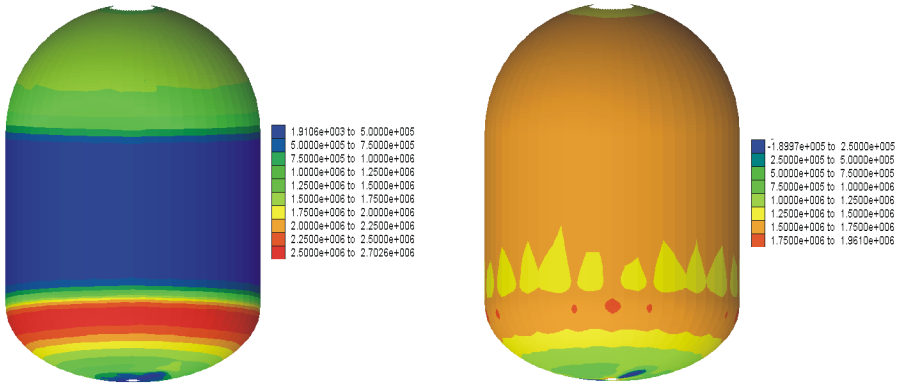

a) vertical force b) horizontal force

Note: To obtain the stress, the force should be divided by steel liner thickness (i.e., 15 mm)

Figure 16 Case 1, 5° Friction Angle Between Steel and Concrete: Forces (MN) in the Steel Liner

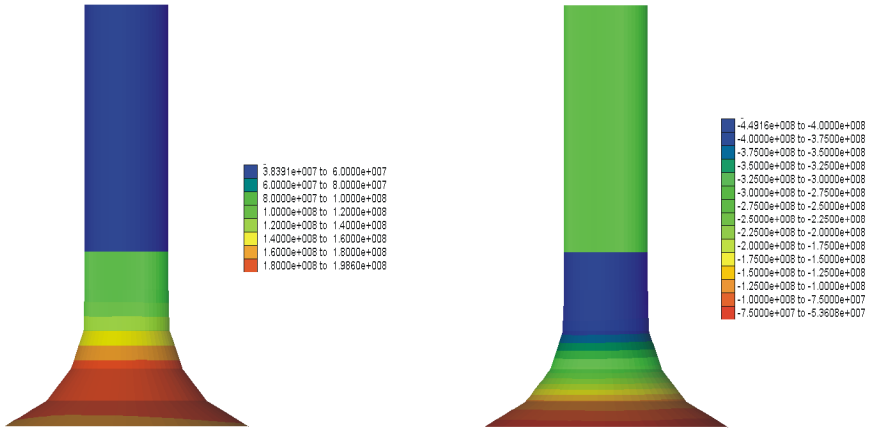

a) major principal stress b) minor principal stress

Figure 17 Case 1, 5° Friction Angle Between Steel and Concrete: Stresses (MPa) in the Production Pipe

5.2.3 Case 2: Continuous, Elastic-Plastic Rock Mass

The stresses in the steel liner of the cavern (Membrane forces are shown in Fig. 18.), assuming no friction between the steel and the concrete, are 150 MPa in the horizontal direction (in the middle of the height of the cavern) and 110 MPa in the vertical direction (in the invert). The maximum strain in the horizontal direction is 0.06%. The stresses in the production pipe (Fig. 19) show that the maximum tension (and, at the same time, the Tresca stress) is approximately 340 MPa, which is less than the allowable stresses (discussed in Section 5.2.1). If a friction angle of 5° is assumed between the concrete and the steel, the maximum tensile stress (and, at the same time, the Tresca stress) is approximately 490 MPa, which is also less than the allowable stress for steel of 500.6 MPa according to the CODAP code, and equal to the allowable stress according to the ASME code.

The results of the analyses for Cases 1 and 2 were supposed to be compared with the results reported by Gaz de France, in Review Document 5. However, because of some overly simplified assumptions used by Gaz de France, the results are quite different. The interaction between the cavern liner and the surrounding rock mass was not correctly accounted for in the analysis reported by the LRC group in Review Document 5. Consequently, in their analysis for loading Case 2, which is also considered in the review discussed in this report, the steel liner inside the production pipe detaches from the concrete. This is certainly an unexpected effect considering that the loading case involves 23-MPa gas pressure inside the cavern and the production pipe. The estimates of stresses in the production pipe obtained by the LRC group, therefore, are incorrect.

Based on the results presented in this section, it appears that the assumption (Review Document 5, p. 4) of a 0° friction angle in the interface between the steel and the concrete is non-conservative with regard to stresses predicted in the production pipe. The analysis demonstrates the importance of the shear resistance of the bituminous layer, particularly for stresses in the production pipe. If the friction angle of the bituminous layer is assumed to be 5°, the stresses in the production pipe could be (depending on the yield stress of the steel and the deformability/strength of the rock mass) over the tolerance limit. (The analysis presented in this report uses a 5° friction angle in the interface, which is certainly, according to Review Document 1, conservative.) Therefore, besides ensuring that the bituminous layer has very low shear resistance during construction, the analysis should take accurate account of the shear resistance. One option would be to consider the time-dependent shear deformation of the bituminous layer (creep) with regard to the time scale of pressure oscillation inside the cavern.

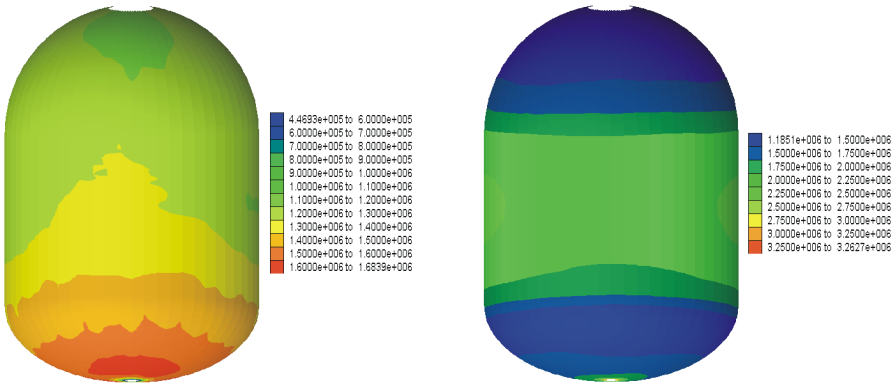

a) vertical force b) horizontal force

Note: To obtain the stress, the force should be divided by steel liner thickness (i.e., 15 mm)

Figure 18 Case 2: Forces (MN) in the Steel Liner

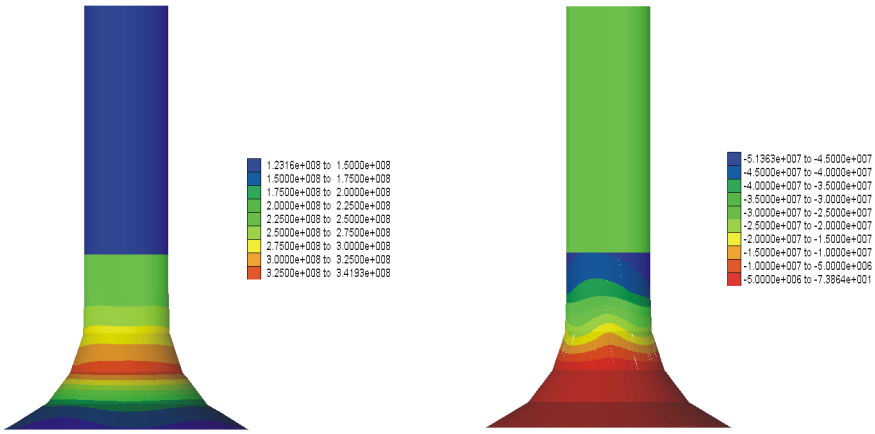

a) major principal stress b) minor principal stress

Figure 19 Case 2: Stresses (MPa) in the Production Pipe

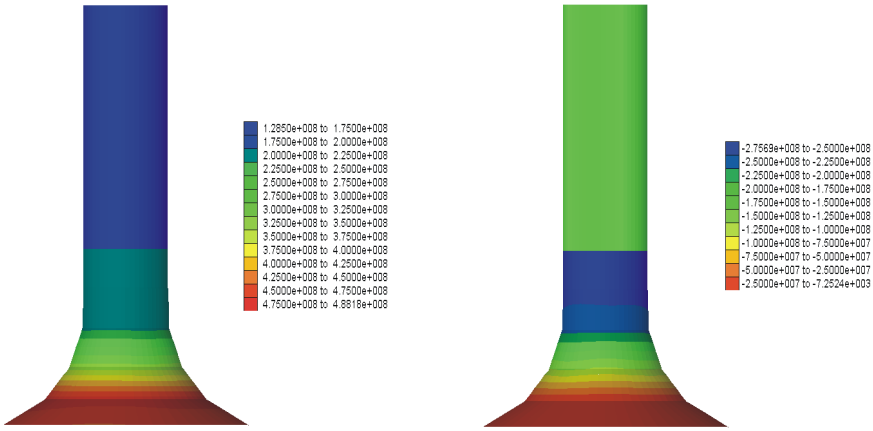

a) major principal stress b) minor principal stress

Figure 20 Case 2, 5° Friction Angle Between Steel and Concrete: Stresses (MPa) in the Production Pipe

5.2.4 Case 4: Discontinuous Rock Mass, Wedge No. 2

Case 4 (discontinuous rock mass, wedge No. 2) results in the most unfavorable stress conditions in the steel liner compared to all other "wedge" cases listed in Table 1 and shown in Figure 3. The major and intermediate principal stresses (The minor principal stress is zero.) for Case 4 (no shear resistance in the interface between the steel and the concrete) due to gas pressure inside the cavern are shown in Figures 21 (in the connection plate) and 22 (in the production pipe). The maximum Tresca stress is approximately 200 MPa, which is less than the limit.

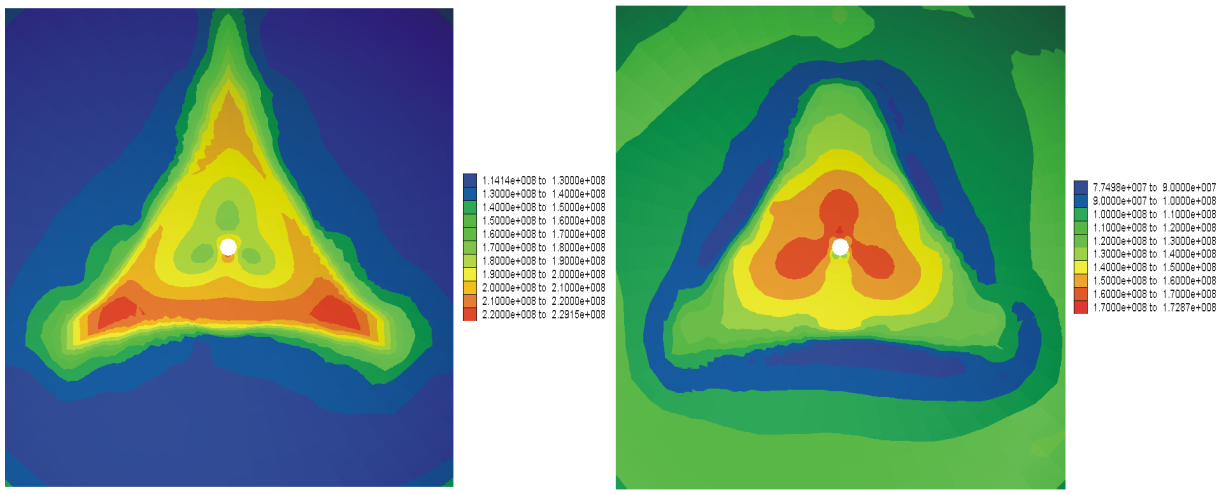

a) major principal stress b) intermediate principal stress

Figure 21 Case 4: Stresses (MPa) in the Connection Plate

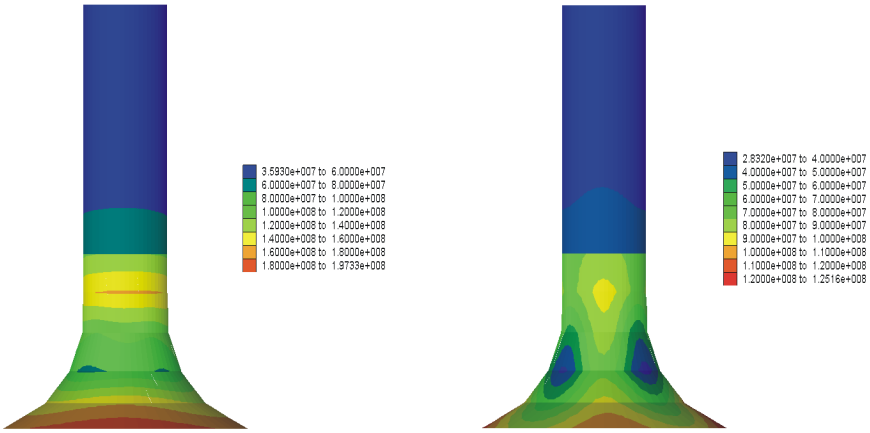

a) major principal stress b) intermediate principal stress

Figure 22 Case 4: Stresses (MPa) in the Production Pipe

However, if shear resistance due to the 5° friction angle is assumed in the interface between the steel and the concrete, the stress and strain conditions are more severe, as shown in Figures 23 and 24. The maximum Tresca stress in the connection plate is 514 MPa; the maximum Tresca stress in the production production pipe is 632 MPa. Both stresses exceed the allowable Tresca limits of 490 MPa (the ASME code) or 500.6 MPa (the CODAP code) but are still less than the limit of 665 MPa according to the CODAP code for a 355-MPa yield stress. The maximum strain in the connection plate is 0.21%.

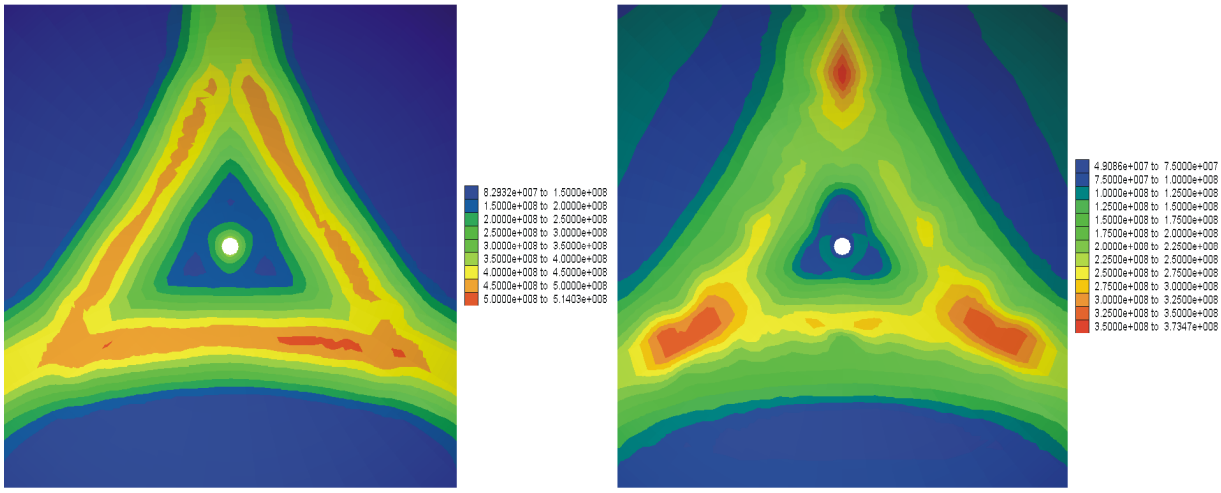

a) major principal stress b) intermediate principal stress

Figure 23 ***Case 4, 5° Friction Angle Between Steel and Concrete: Stresses (MPa) in the Connection Plate***

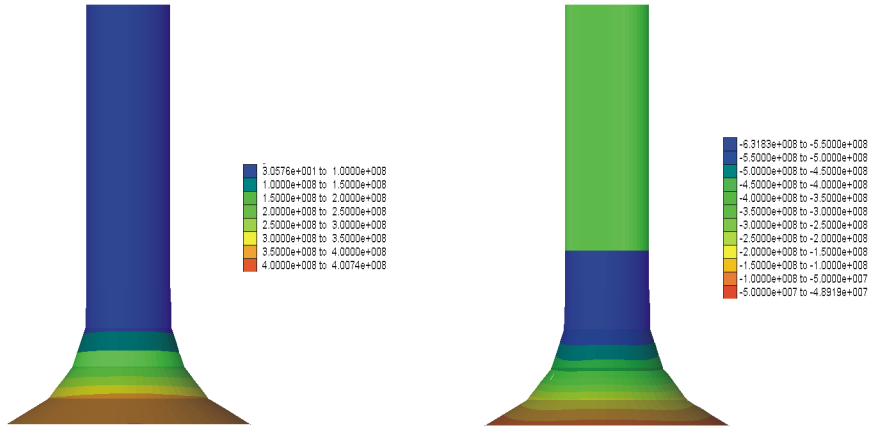

a) major principal stress b) minor principal stress

Figure 24 ***Case 4, 5° Friction Angle Between Steel and Concrete: Stresses (MPa) in the Production Pipe***

5.2.5 Case 13: Discontinuous Rock Mass, Joints No. 13

Case 13 (discontinuous rock mass, joints No. 2) results in the most unfavorable stress conditions in the steel liner compared to all other "joint" cases listed in Table 1 and shown in Figure 4. The calculated stresses in the cavern, connection plate and the production pipe for the case with no friction resistance are shown in Figures 25 through 30. The maximum Tresca stress in the cavern and the connection plate is 465 MPa. The maximum Tresca stress in the production pipe is of the order of 700 MPa, which is certainly over the limit even for the case of 355-MPa yield stress.

The results for the 5° friction angle in the interface again show much larger localized strains and stresses. For example, the maximum Tresca stress in the cavern liner is 766 MPa. The maximum strain is 0.31%, which is still in the domain of high-cycle fatigue, but close to the limit for low-cycle fatigue. The maximum Tresca stress in the production pipe is 670 MPa, more than the limit for a 355-MPa yield stress for steel.

Jointing conditions (for both wedge and jointing cases) are selected arbitrarily. However, the considered cases represent conditions that are certainly possible at potential future LRC sites. The analysis shows that those unfavorable conditions can lead to high stress/strains in the steel liner, particularly inside the production pipe. Stresses inside the liner of the production pipe for Case 13 are larger than the allowable stresses even if no shear resistance is assumed in the bituminous layer. Conditions become worse for the 5° friction angle in the bituminous layer: almost all cases considering a discontinuous rock mass predict Tresca stresses in the steel liner of the production pipe above the allowable limit. However, even the maximum strains for the most unfavorable conditions (discontinuities, friction) remain within the limit of the high-cycle fatigue.

It is clear that the effect of discontinuities on the deformation of the steel liner should be considered carefully both during the construction and the design. Discontinuities should be considered explicitly and as accurately as possible in the analysis. Any other approach (e.g., continuum, smeared cracks) can lead to either unsafe or overly conservative design.

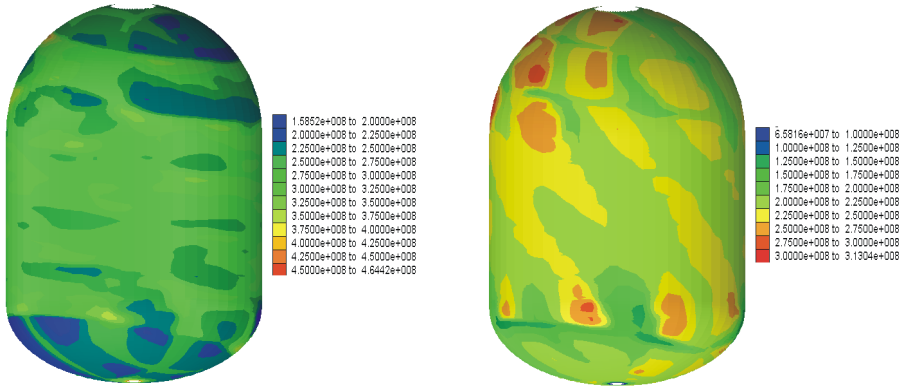

a) major principal stress b) intermediate principal stress

Figure 25 Case 13: Stresses (MPa) in the Cavern

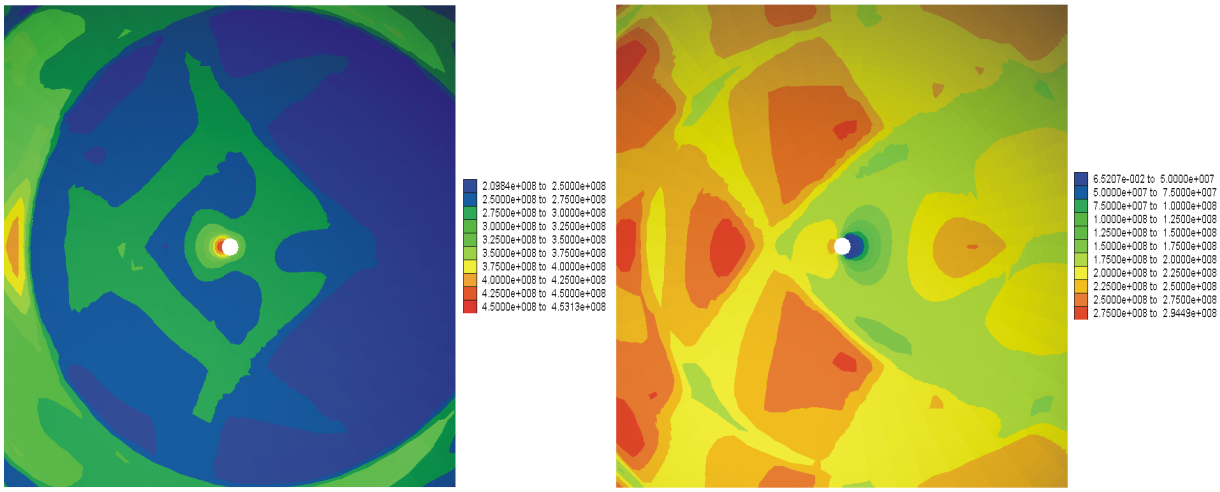

a) major principal stress b) intermediate principal stress

Figure 26 Case 13: Stresses (MPa) in the Connection Plate

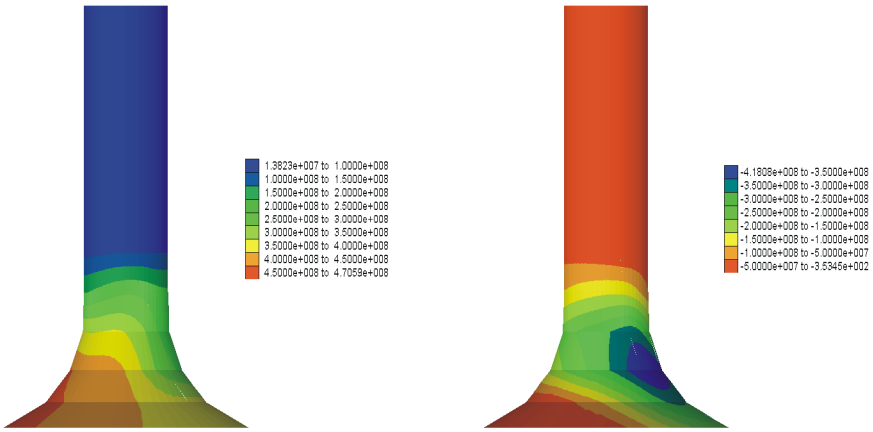

a) major principal stress b) minor principal stress

Figure 27 Case 13: Stresses (MPa) in the Production Pipe

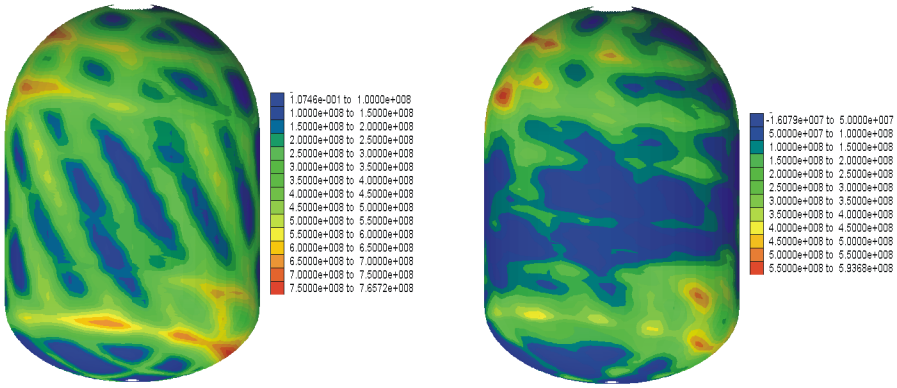

a) major principal stress b) intermediate principal stress

Figure 28 Case 13, 5° Friction Angle Between Steel and Concrete: Stresses (MPa) in the Cavern

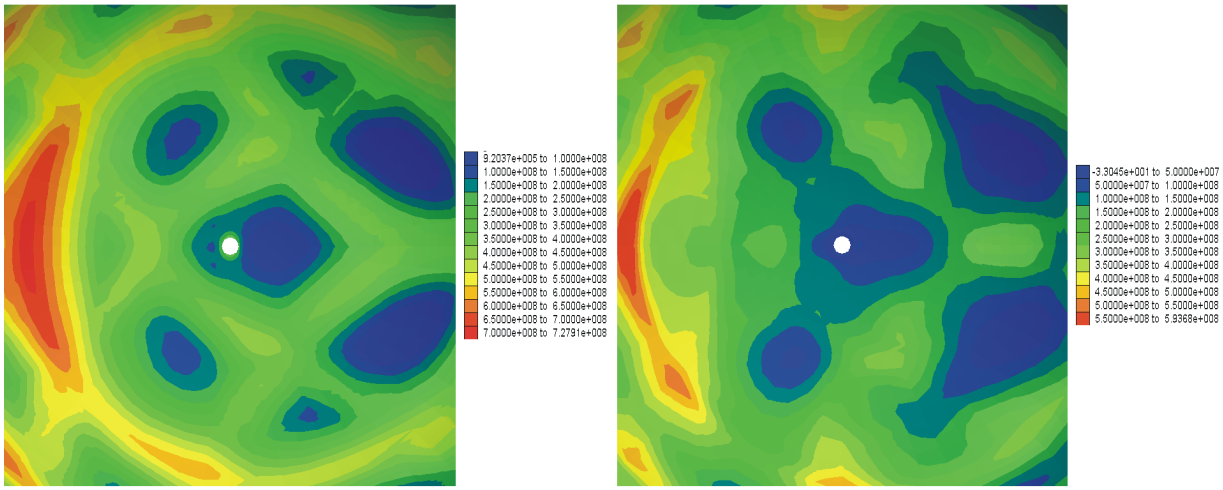

a) major principal stress b) intermediate principal stress

Figure 29 Case 13, 5° Friction Angle Between Steel and Concrete: Stresses (MPa) in the Connection Plate

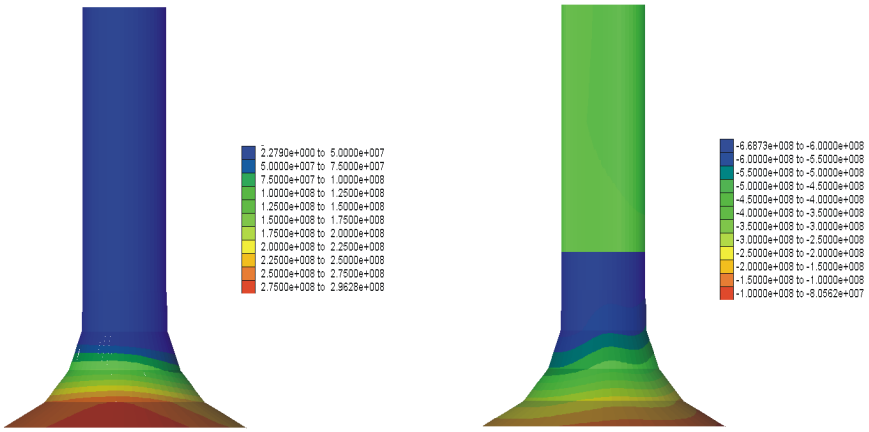

a) major principal stress b) minor principal stress

Figure 30 Case 13, 5° Friction Angle Between Steel and Concrete: Stresses (MPa) in the Production Pipe

5.2.6 Effect of Cyclic Loading

The strain range during operation cycling was investigated. Five cycles of gas pressure oscilations between 23 MPa and 3 MPa were simulated in the numerical model for Case 4 (discontinuous rock mass, wedge No. 2). The calculated evolution of cavern deformation during the first 3 cycles is shown in Figure 31. As expected, a significant portion of initial wedge displacement is irreversible. Consequently, the maximum strain (0.21% in the first loading) is 0.186% or less in the subsequent loading cycles. Since the residual gas pressure in the cavern is 3 MPa, strain range in the loading-unloading cycles following the first cycle is 0.144% or less.

It appears from these results that the effect of discontinuities in the rock mass on the maximum stress/strain in the steel line is reduced significantly during subsequent cycles compared to the effect in the first cycle. The reason for this is the irreversibility of a significant portion of the initial deformation (during the first loading) of discontinuities in the rock mass. Basically, the blocks settle in place during the first cycle.

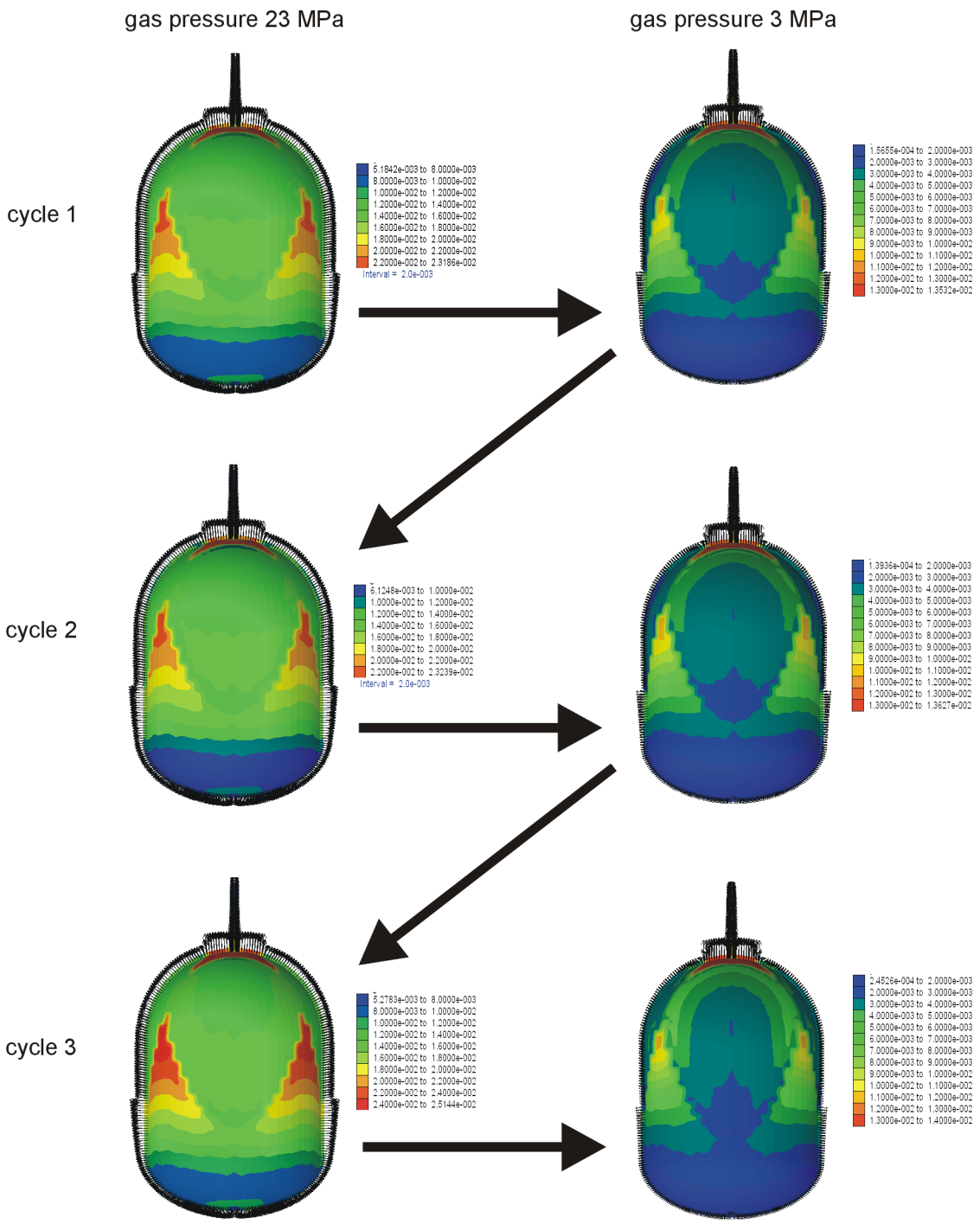

Figure 31 ***Case 4: Displacement Vectors and Contours of Displacement Magnitude (m) Due to First 3 Loading Cycles***

6.0 FATIGUE AND CRACK GROWTH

This section summarizes the findings from the review of the documents referenced in Section 3.1 regarding the fatigue and fracture of the steel liner for a proposed Lined Rock Cavern. The objective was to review the fitness-for-purpose evaluations (described in the review documents) and to examine the liner with respect to codes that will govern the construction and operation of a LRC in the United States. The primary concern regarding the liner is fracture from crack-like welding discontinuities, or propagation of these cracks by low-cycle fatigue (A cavern will undergo approximately 500 cycles in its lifetime.), eventually leading to leaking of the liner or fracture.

It is understood that the liner is made from low-alloy structural steel plates 12 mm to 15 mm thick with a minimum specified yield strength of 355 MPa and a minimum Charpy requirement of 30 Joules at -40° C. According to Review Document 1, the plates are joined with complete joint penetration groove welds backgouged and welded from the second side.

There is one special weld (the last weld according to page 95 of Review Document 1) that will have to be made from one side only and which will have a backing bar remaining. This weld will be located in an area of lower strain demand (according to Review Document 1) and, therefore, is not critical and will not be discussed further.

The construction drawings (Review Document 9) also show several potentially important details that are not discussed in the review documents, such as Detail A in Drawing No. 669-024 Rev. C of Review Document 9, shown in Figure 32, which is a transition from a 324-mm diameter pipe to the liner. However, the detail that appears most critical is Detail D in Drawing No. 669-025 Rev. B of Review Document 9, shown in Figure 33, which includes a pipe foot and a gusset-plate attachment fillet-welded to the liner. This detail will have a stress concentration greater than 4, and therefore it is essential that this location at the bottom of the liner also is a location of reduced stress and strain ranges.

The internal pressure on the liner, according to Review Document 2, ranges from 3 MPa to 20 MPa. The minimum temperature at the maximum pressure is 10° C. According to page 5 of Review Document 1, the nominal membrane strain range (not considering the effect of the stress concentrations at the details) is estimated to be in the range between 0.1% and 0.2%. (In many other places in the report, lower strain ranges — typically 0.1% or less — are discussed.) This is approximately equal to the yield strain, which is 0.17%. Therefore, it is realistic to expect the peak stress to equal the minimum specified yield strength, 355 MPa. The stress range of 218 MPa (e.g., Review Document 1, p. 98) was used in the fatigue analysis. The stress range was derived (Review Document 1, p. 94) from the 98-percentile strain range of 0.089%, obtained from the probabilistic design approach.

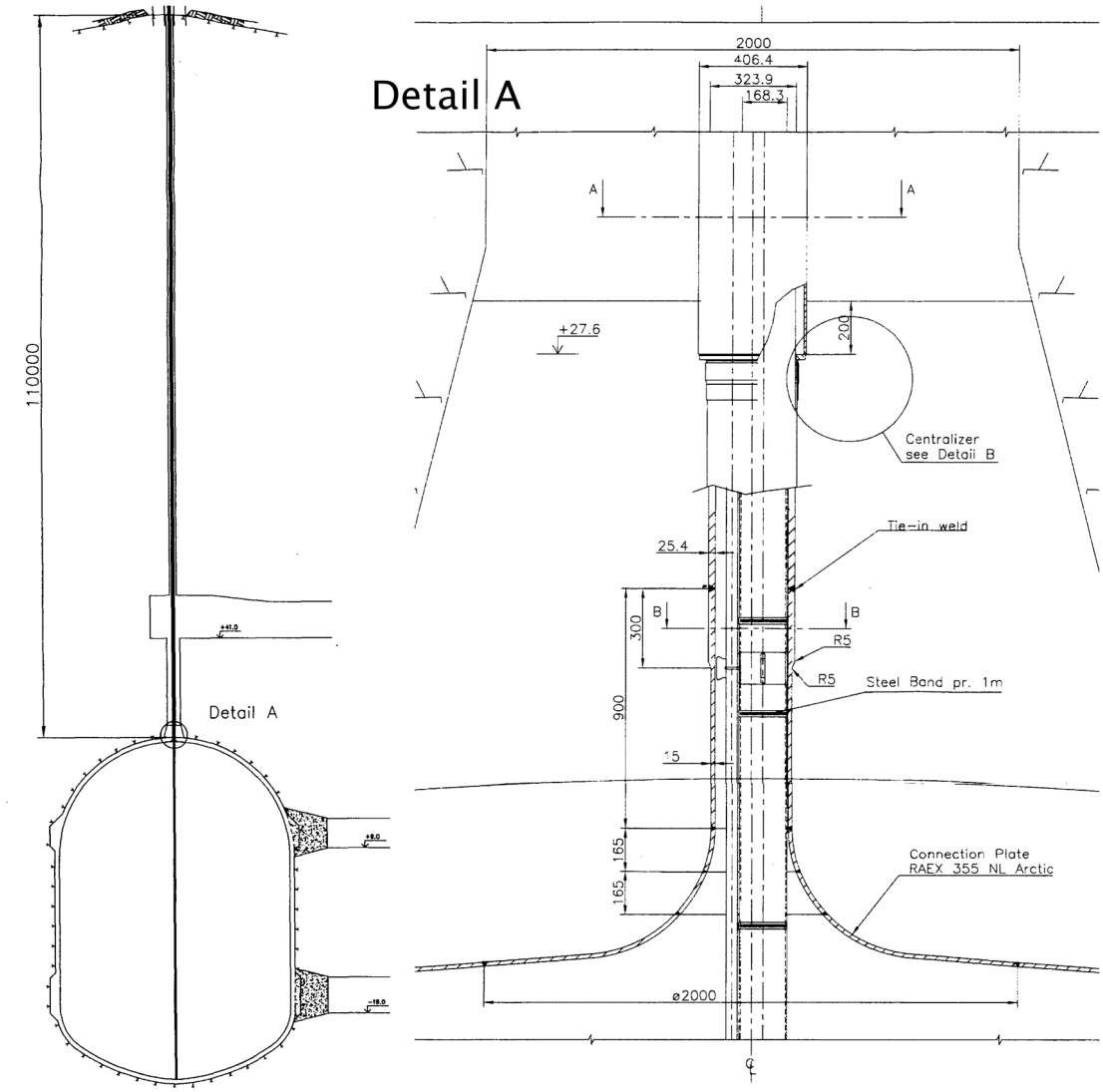

Figure 32 Detail of Transition From the Production Pipe to the Liner

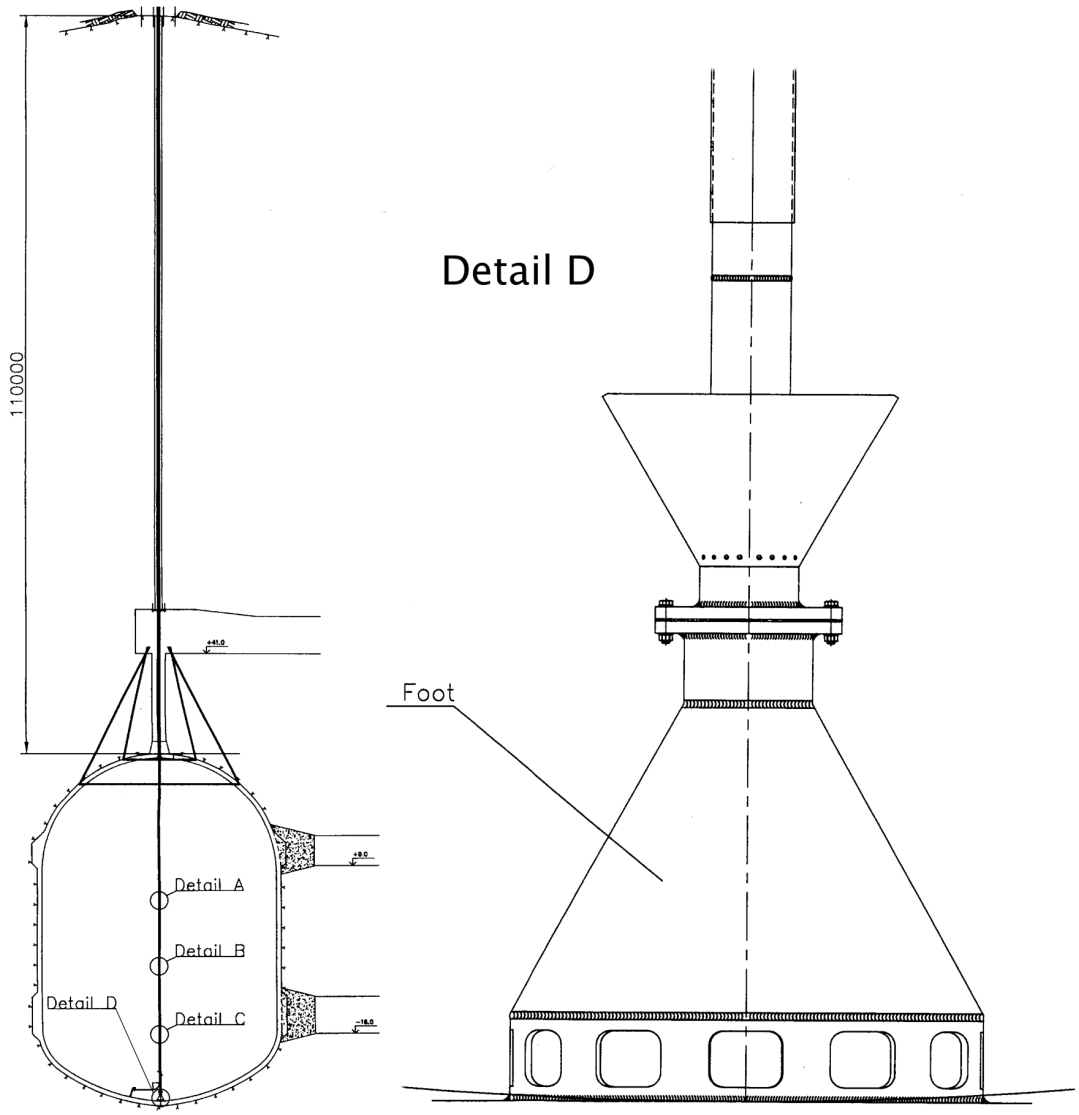

Figure 33 Detail of the Pipe Foot

6.1 Initial Defect Size

The welds will be 100% inspected with ultrasonic testing, and 10% randomly tested with radiographic testing. In addition, the surfaces of the welds will be inspected using either magnetic-particle or dye-penetrant techniques. Despite this rigorous weld testing, the welds will be fabricated with the typical minor defects and discontinuities that are present in all welded-steel structures. In the United States, the results of the inspection will likely be evaluated by the standards of American Welding Society (2000): AWS D1.1 , "Structural Welding Code - Steel". AWS D1.1 is widely applied as a workmanship standard for new construction of a variety of steel structures. Welds with defects and discontinuities that do not meet the standards of AWS D1.1 must be repaired and retested. Therefore, the worst-case flaws for consideration in the fitness-for-purpose evaluation are the types and sizes of defects that are acceptable according to AWS D1.1. Every detail of the structure should be evaluated with respect to brittle fracture, fatigue and crack growth, assuming that worst-case defect is present right after the inspection, although it is very likely that the maximum discontinuities in most members are far smaller. Table 4 summarizes the worst-case defect sizes.

Table 4 Summary of Worst-Case Defects

Type of defect	Relevant AWS provisions	Maximum defect size
Undercut	Table 6.1	0.25 mm in primary member
Crack at attachments	5.26.1.4	0.025 mm
Buried defects 15 mm thick	Figure 6.1	10 mm
Buried defects 12 mm thick	Figure 6.1	8 mm

Undercut — The standards for acceptance of weld undercut are found in Table 6.1 of AWS D1.1. For transverse butt welds in primary tension members, the undercut must be less than 0.25 mm.

Crack at Attachments — The requirements for cracks are provided in Section 5.26.1.4 of AWS D1.1, which states that cracks must be repaired. The worst-case defect size is theoretically zero, because cracks are not allowed in AWS D1.1. However, it is conceivable that a crack as large as the surface roughness for a torch-cut surface could be tolerated. Therefore, the worst-case defect size for a crack at an attachment in Table 4 is assumed conservatively to be 0.025 mm.

Buried Defects — The standards for acceptance of buried defects by ultrasonic testing (UT) are given in Section 6.13 of AWS D1.1. Table 6.2 of AWS D1.1 presents the criteria for statically loaded non-tubular connections. For the thickness of the liner (less than 20-mm thick) the dB rating of any indications must be:

1. greater than +8 for long indications greater than 50 mm;
2. greater than +7 and not more than 50 mm long;
3. greater than +6 and not to exceed 20 mm long;

4. greater than +5 for any length.

On many occasions, the section indicated as having a rejectable dB rating will be cored out of a groove weld for destructive examination and characterization of the actual flaw. Figure 34 shows the results of many of these investigations plotted in terms of the dB rating versus the largest dimension of the actual flaw size. The AWS D1.1 rejection limits for butt welds of various thicknesses are also shown in the figure. It can be seen that the AWS criteria are very conservative. For the liner less than 19 mm thick, the +5 dB rating ensures a defect size less than 1 mm in diameter.

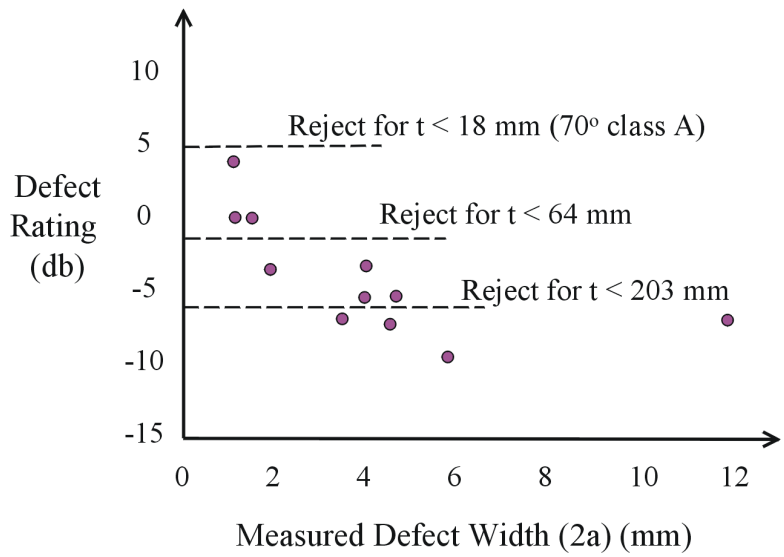

Figure 34 Actual Defect Size From Destructive Examinations of Cores From Welds With UT Indications of Various dB Ratings

Because the AWS acceptance criteria for UT are not quantitative in terms of the size of the defect, it is useful to examine the acceptance criteria for radiographic testing (RT). It is assumed that the UT acceptance criteria are calibrated to achieve about the same quality level as the RT acceptance criteria. The RT acceptance criteria are given in Figure 6.1 in AWS D1.1, and they vary with thickness of the weld. The appropriate worst-case defects from Figure 6.1 in AWS D1.1 for the thicknesses of the critical members considered for LRC are given in Table 4. The values in the table represent the largest dimension across the defect. (The defects are usually elongated following the weld beads; the dimension in Table 4 is the total length of this defect.) The buried defects should be modeled as perfectly round cracks with diameters as large as the worst-case defect dimension in Table 4, which is certainly conservative. It can be seen that these acceptance criteria are much more liberal than the destructive testing of the UT indications shown in Figure 34.

According to the discussion on page 107 of Review Document 1, the welds should be inspected to "Level BV, stringent requirements according to ISO 5817". Consequently, the maximum remaining defect would be a 3-mm diameter buried defect. In analyses of crack propagation in Review Documents 2 and 3, an initial semi-circular surface crack with a depth of 3 mm and a surface length of 6 mm is assumed. This assumed defect size is twice the size of the 3-mm diameter defect discussed in Review Document 1 and is also surface-breaking, which makes this assumption very conservative. In Review Document 3, a through-thickness crack of 3 mm in length is also evaluated. As can be seen by comparison of these assumptions to the AWS maximum allowable flaw sizes in Table 4, the assumed surface crack size is very conservative.

The buried cracks were neither evaluated nor discussed in the review documents. A buried crack somewhat larger than defects discussed in Review Document 1 is possible according to AWS D1.1. However, buried defects are much less severe than edge cracks and are not expected to be an issue with regard to the fatigue and fracture of the steel liner.

6.2 Fracture Mechanics Analysis

Weld defects can develop into cracks and propagate by fatigue when subjected to repeated loading and unloading. The liner will be subjected to up to 500 large stress ranges, approximately equal to the yield strength. Using established fracture-mechanics principles, acceptable initial crack size can be defined as a crack size that will not propagate to the critical size in the lifetime of the structure being considered. These types of calculations are referred to as fitness-for-purpose analyses, indicating that, although a component may have defect or discontinuity, it can be proven that it is fit for its defined purpose (lifetime and anticipated loading). The British Standards Institute (1999) published a document entitled: "Guide on Methods for Assessing the Acceptability of Flaws in Metallic Structures" (BS7910), which outlines a detailed procedure for a fitness-for-purpose analysis. BS7910 is applicable to a broad range of structures, including the liner, and has been used for decades. It is recommended that the liner be evaluated using the established procedures of BS7910. The result of this evaluation would be the maximum allowable defect size. If this allowable defect size is greater than the worst-case defect size allowable under AWS D1.1 (Table 4), then the structural capacity will not be affected by the defects.

The calculations in BS7910 are based on linear elastic fracture mechanics (LEFM). The calculations involve the stress-intensity factor (K), which characterizes the stress field at notches or cracks. Crack-like notches and weld defects are idealized as cracks, and the term crack will be used to include crack-like notches and weld defects. The applied K is determined by the size of the crack and the nominal gross-section stress remote from the crack. BS7910 presents solutions for the applied stress-intensity factor, K, for a variety of geometries. The following discussion outlines a few useful solutions and examples of their application to welded joints.

In general, the applied stress-intensity factor is given as

$$K = F_c \times F_s \times F_w \times F_g \times \sigma\sqrt{\pi a} \tag{2}$$

where the F terms are modifiers on the order of 1.0, specifically:

F_c is the factor for the effect of crack shape,

F_s is the factor, equal to 1.12, that is used if a crack originates at a free surface,

F_w is a correction to account for a finite size of a structure because the basic solutions were generally derived for infinite or semi-infinite bodies, and

F_g is a factor for the effect of non-uniform stresses, such as a stress concentration or a bending stress gradient.

A stress concentration factor (SCF) is defined as the ratio of the peak stress near the stress raiser to the nominal gross-section stress remote from the stress raiser. SCF is often used in fracture assessments when the crack is located near a stress raiser. For example, if a crack is located at the edge of one of the fillet-welded attachments, the SCF will be between 4 and 5. SCF is included in F_g. The stress intensity factor has units of MPa·m$^{1/2}$.

The fracture toughness, called K "critical" or K_c, is a material property characterized in terms of the applied K at the onset of fracture in simplified small test specimens. The fracture toughness, K_c, is considered a transferable material property — i.e., fracture of structural details is predicted if the value of the applied K exceeds K_c.

6.3 Toughness Testing

In the United States, the Charpy test is the accepted way of specifying toughness for structural steel. It is our opinion that the fracture mechanics testing described in Review Document 4 is not required in order to ensure adequate toughness of the steel liner plate or filler metal. The Charpy test ensures a certain level of toughness.

The liner could be designed in accord with the American Institute of Steel Construction's (AISC) "Load and Resistance Factor Design Specification for Structural Steel Buildings" (2000). Current AISC specifications refer to American Society for Testing and Materials (ASTM) specifications for structural steel, such as A36 (2001a). Without supplemental specifications, these steel specifications do not require the Charpy test to be performed. Therefore, the Charpy V-Notch (CVN) impact test must be specified by the purchaser of steel as a supplemental requirement.

ASTM A673 (2001b) has specifications for the frequency of Charpy testing. The H frequency requires a set of three CVN specimens to be tested from one location for each heat or about 50 tons. These specimens can be taken from a plate with thickness up to 9 mm different from the product thickness if it is rolled from the same heat. The P frequency requires a set of three specimens to be tested from one end of every plate. The steel specifications for the steel liner should require CVN testing at the P frequency.

Due to variability in the cooling rate and resultant microstructure and grain size, toughness of a weld metal can vary widely depending on manufacturer's certification, weld-procedure qualification testing, and the fabrication of the structure. The toughness is dependent on proper shielding gas and flux to reduce impurities. Therefore, welding procedures must be monitored to control toughness as well as to avoid defects. Typically, higher heat input decreases cooling rate and toughness. Qualification tests are often carried out on plates 25-mm thick. The procedure may then be applied to thinner plates, where cooling rates will decrease and the toughness may be lower than qualification tests indicate. Therefore, it is recommended that the weld-procedure qualification tests, including the CVN tests, be performed periodically for every welder on the job using plates of the same thickness of the liner.

6.4 Estimation of Toughness

A widely accepted correlation for the lower shelf and lower transition region between K_c and CVN is credited to Barsom and Rolfe (1987):

$$K_c = 11.5 \times \sqrt{\text{CVN}} \tag{3}$$

where CVN is given in J, and K_c is given in MPa·m$^{1/2}$. (A different constant is used for English units.) Figure 35 shows K_c data for a variety of brittle materials that have caused fractures of steel structures in the past (Barsom and Rolfe 1987). Data from the web/flange core region of a W14×605 "jumbo" wide-flange column section are shown. This material in the core region of jumbo sections made in the past had unusually low toughness and caused several fractures in the early 1970s, when the shapes were used as tension chords in trusses. The lower-bound CVN energy for the core region ranges from 4 J to 14 J. Using the correlation of Equation (3), the scatterband for the predicted K_c ranges from 23 MPa·m$^{1/2}$ to 43 MPa·m$^{1/2}$. The scatterband for K_c based on the Charpy data is shown in Figure 35 with measured K_c data from fracture mechanics tests. These data show that the correlation of Equation (3) is conservative, as the actual K_c ranges between 45 MPa·m$^{1/2}$ and 50 MPa·m$^{1/2}$.

Also shown in Figure 35 are K_c data calculated, using Equation (3), from the CVN data measured for several brittle welds that caused fractures in the past. One example is the brittle self-shielded flux-cored arc welds that were used in moment-frame connections prior to the Northridge earthquake in 1994. Another is the brittle welds that caused a fracture, in January 1986, of a steel box section supporting a roof at the Wolf Trap Outdoor Performing Arts Center in Virginia. It happens that the values of CVN and K_c for these brittle welds also fall within the scatterband for "lower-shelf" brittle-fracture-prone materials, as shown in Figure 35. The lower bounds of the CVN and K_c data are not sensitive to temperature or strain rate because these materials do not undergo a transition at temperatures of interest. This similarity in the data suggests that a there may be a lower-bound value of the fracture toughness that can be assumed for brittle ferritic weld metal, structural steel and the heat-affected zone (HAZ). The lower-bound fracture toughness reflects the worst effects of temperature and strain rate. For these conditions and materials, the lower-bound fracture toughness is about 50 MPa·m$^{1/2}$. Because the data in Figure 35 are characteristic of the most brittle steel and

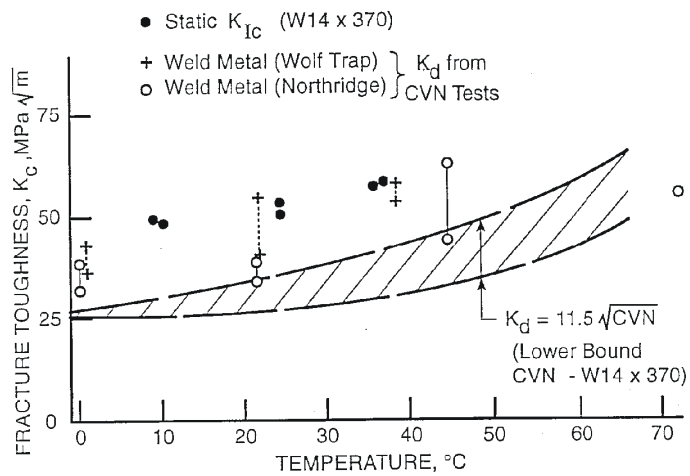

Figure 35 Fracture Toughness Data for a Number of Brittle Materials That Have Caused Fractures in the Past

weld metal that have ever been used in the past, a minimum fracture toughness of 50 MPa·m$^{1/2}$ can be conservatively assumed for the steel, weld metal, and HAZ in the liner as well. Using Equation (3), it can be shown that 50 MPa·m$^{1/2}$ corresponds to a minimum Charpy value of about 19 J at the lowest anticipated service temperature. BS7910 has a slightly different correlation for the use of Charpy to predict fracture toughness that also depends on the thickness of the plate. Using CVN equal to 19 J, the correlation in BS7910 gives a fracture toughness of 58 MPa·m$^{1/2}$ for sections 10-mm thick, and 50 MPa·m$^{1/2}$ for sections 25-mm thick. Thus, this correlation essentially gives the same result.

As discussed previously, the steel for the liner should have a minimum Charpy requirement of 30 J at -40° C. This requirement corresponds to a K_c of 63 MPa·m$^{1/2}$. However, the minimum operating temperature at maximum pressure is 10° C, so the Charpy at this temperature would be expected to be much greater. On page 4 of Review Document 2, experimental values of 65 J (corresponding to K_c of 93 MPa·m$^{1/2}$) are discussed. Furthermore, there is a strain rate shift that would make the K_c value much greater than would be obtained from Equation (3). In Review Documents 1 and 3, K_c was taken as 80 MPa·m$^{1/2}$. In Review Document 2, K_c was taken as 127 MPa·m$^{1/2}$, but the maximum applied K was compared to 0.7 times K_c, or 90 MPa·m$^{1/2}$. These assumptions seem entirely reasonable and conservative. However, it should be ensured that the steel plate used to make the liner meets these minimum requirements. The new data on fracture toughness testing provided in Review Document 4 support the use of a critical fracture toughness as high as 244 MPa·m$^{1/2}$. However, these high values characterize particular steel and weld material. There is no reason to believe that the same materials will be used in the United States.

6.5 Critical Defect Size

Slightly different approaches are used in the review documents for calculating the critical final crack size. Because there is no equivalent U.S. standard, it is recommended that fracture assessments be conducted in accordance with BS7910, which is widely accepted in the oil and gas industry as well as in many other industries. The review documents use a failure-analysis diagram approach, which basically augments the LEFM approach, to include a check of possible plastic limit load. This is essentially the same as the approach in BS7910.

However, there is an inconsistency in calculated critical defect sizes as presented in the review documents. The results obtained in Review Documents 1 and 3 conculde that a through-thickness crack of 10.5 mm, as well as a surface crack 9.1 mm in length and 4.6 mm deep, could be tolerated. The critical defect sizes reported in Review Document 4 are larger: 5.4-mm critical crack depth, 10.8-mm surface length, and 98.5-mm critical length of the through-thickness crack. The increased length of critical defect reported in Review Document 4 is supposedly a consequence of the larger fracture toughness used (i.e., $K_{Ic} = 244$ MPa·m$^{1/2}$ compared to $K_{Ic} = 80$ MPa·m$^{1/2}$ used in Review Documents 1 and 3). Assuming that the critical defect size is calculated based on augmented LEFM, the increase in the critical defect size should be proportional to the square of the ratio of fracture toughnesses. Consequently, the increase in the critical length of the through thickness crack from 10.5 mm to 98.5 mm seems correct. However, the increase in critical length of surface cracks from 9.1 mm to 10.8 mm when toughness is increased from 80 MPa·m$^{1/2}$ to 244 MPa·m$^{1/2}$ seems unreasonable.

Review Document 2 also described a tearing instability analysis using a J-R curve. This is a more sophisticated analysis, and showed that a slightly larger crack size could be tolerated. However, the tearing analysis was based on only estimated lower-bound material properties, so it is not necessarily expected to be more accurate.

6.6 Secondary Stresses in Fracture Assessments

BS7910 requires that any secondary stress, such as weld residual stress, also be included in the calculations of the stress intensity factor, K. In this case, the applied K might be as high as twice the value computed using a peak stress equal to the 355-MPa yield stress of the plate, because the residual stress could also be as high as 355 MPa. This requirement of BS7910 is not considered in the review documents.

In terms of stress, this approach seems overly conservative. However, the simplified Level 1 fracture analysis procedure in BS7910 actually is derived from a strain-based procedure known as the CTOD design curve. This design curve was derived empirically from full-scale tests on wide plates with transverse butt welds. In this procedure, the strains from primary and secondary stresses were added together to calculate the strain demand on the wide-plate tests. Although it is conservative and based on the lower bound to these full-scale tests, it is consistent with the data. Therefore, the other approaches that did not include secondary stresses are somewhat insufficient in this regard.

Note that although residual and other secondary stresses should be included in the fracture part of the assessment, they are not supposed to be included in the plastic limit load calculations. This is due to secondary stress shakedown as the plastic limit load is approached. Therefore, including residual stresses has an effect on the potential for brittle fracture only, and it is appropriate to be as conservative as practical when it comes to avoiding brittle fracture. Residual stresses and other secondary stresses should not be included in the assessment of low-cycle fatigue.

It is clear that secondary stresses should be included in the fracture assessment. However, taking the full value of the plate yield strength as an estimate of the residual stress is very conservative. BS7910 has provisions for more sophisticated analyses (Level 2 and Level 3) where more refined estimates of the residual stress are used. However, these approaches require material properties for the actual steel and filler metal being used. Before the materials are delivered, K is estimated from the Charpy requirements, and only the Level 1 procedure is appropriate. It is believed that, despite the more conservative assumptions, the Level 1 procedure will still show that the maximum defects allowed by AWS D1.1 are acceptable and will not present a significant risk of fracture.

6.7 Low-Cycle Fatigue

There are several approaches used in Review Documents 1, 2 and 3 to assess the possibility of crack formation by low-cycle fatigue. Review Document 1 begins with a classical strain-life equation (Manson equation, developed from tensile test data) that suggests an allowable strain range of 2% for 500 cycles. Then, a lower-bound strain-life relation is examined that suggests an allowable strain range of 0.5% for 500 cycles. Next, Review Document 1 treats the problem with the high-cycle fatigue S-N approach, using an S-N curve for intersecting butt welds. This S-N curve has a fatigue strength of 80 MPa at 2 million cycles. For the elastic stress range of 219 MPa, this approach gives a life of 39,000 cycles. Although not used this way in Review Document 1, this approach could also be used to predict an elastic stress range at 500 cycles, which would be about 1270 MPa. This would correspond to a strain range of about 0.6%. Although this approach seems much different than the strain life equations, it gives a result that is approximately the same. A slightly more conservative approach could be taken if the filet-welded attachments are considered. The S-N curve for these details (AWS Category E) has fatigue strength of 56 MPa at 2 million cycles. This S-N curve predicts an elastic stress range at 500 cycles of 890 MPa. This would correspond to a strain range of about 0.4%. In addition to the welded attachments, this detail category would also include welds with backing bars or even severely corroded areas of the liner, so these would also have an allowable strain range of 0.4%. It is also worthwhile to compare these analyses to the fatigue design rules of the American Society of Mechanical Engineers (ASME), Boiler and Pressure Vessel Code (1998b), Section VIII, Division 2 - Alternative Rules. The appropriate S-N curve, Figure 5-110.1, shows an allowable elastic stress range of 1380 MPa for 500 cycles, corresponding to a strain range of 0.67%. The ASME approach provides fatigue strength reduction factors (FSRF) for the welded details, which are analogous to stress concentration factors (SCF). The butt welds should have a FSRF of about 3, leading to an allowable strain range of about 0.22% for 500 cycles. Note that this is much less that the 0.6% allowable strain range computed using the high-cycle S-N curve for intersecting butt welds. The fillet-welded details have a FSRF of about 4.5, leading to an allowable

strain range of only about 0.15% for 500 cycles. Again, this is much less than the high-cycle S-N curves would allow and shows that the ASME approach is more conservative in this range of cycles. The allowable strain range of 0.15% is very close to the estimated maximum strain ranges in the liner and, therefore, may be of concern. This calculation also shows the importance of these fillet-welded details, which can dramatically reduce the allowable strain range.

6.8 Fatigue Crack Initiation Propagation

The Paris Law (Paris and Erdogan 1962) relating the range in stress-intensity factor (ΔK) to fatigue crack-growth rate (da/dN) is used in BS7910. The Paris Law is expressed as

$$\frac{da}{dN} = C \times (\Delta K)^m \tag{4}$$

where a = crack size,
N = number of cycles,
C = an experimentally determined coefficient,
ΔK = stress intensity factor range, and
m = material constant.

BS7910 gives the value of C and m for steel in a marine environment equal to $1.65 \cdot 10^{-11}$ and 3, respectively, for a in meters and K in MPa·m$^{1/2}$. This is slightly larger and more conservative than the values used in Review Document 2. However, Review Document 3 used the ASME crack growth-rate law that, at 20 MPa·m$^{1/2}$, gave a growth rate 7 times faster than the rate in BS7910. In any case, the maximum crack extension was about 1.3 mm on the surface and 0.5 mm through the thickness for the 355 MPa stress range and 500 cycles.

7.0 STANDARDS OF CONSTRUCTION

Review Document 6 is a comprehensive set of performance requirements for the overall design of the steel liner, required documentation, material requirements for steel plate and filler metal, erection and welding, and inspection. With adaptation for use in the United States, it is sufficient to provide a reliable level of quality that will ensure that the structure can perform as expected.

Much of the material in Review Document 6 is duplication of what would be provided by reference to other codes and specifications, as explained below. The main problem is that it is written for use in Sweden and references Swedish standards. It will need to be rewritten to reference and avoid duplication with appropriate standards in the United States. The primary issues that need adaptation are:

1. design code;
2. available materials (steel plate and filer metal); and
3. construction practice and welding procedures.

7.1 Design Code

The LRC Demo Plant is not a typical structure, and it is not clear what code or standard would govern the design. The applicable code or standard depends on the location and governing federal and/or local regulations.

American Petroleum Institute (API) standards may apply because the purpose of the cavern is to store natural gas. The steel liner is essentially a pressure vessel and, therefore, could possibly be designed by the ASME Boiler and Pressure Vessel Code (1998b). However, the ASME Boiler and Pressure Vessel Code is very prescriptive and assumes that the structure being designed is a conventional pressure vessel. The liner is quite different from a conventional pressure vessel, as the steel liner acts in combination with the concrete and rock to withstand the internal pressure. (Actually, the steel liner only provides the tightness; the pressure is carried by the rock mass.) Also, the ASME Boiler and Pressure Vessel Code allows for specific materials only, whereas there are better materials, not recognized by the ASME Code, that should be used as a steel liner.

One advantage of the ASME Code is that it does have explicit criteria for low-cycle fatigue, which is expected to be the limit state for the liner. The ASME Boiler and Pressure Vessel Code criteria are known to be very conservative, and they would only allow a strain range of about 0.22% for 500 cycles, which could be exceeded in the liner, depending on the assumptions. As discussed in Section 6.0, there were several other low-cycle fatigue analyses performed by other agencies using other criteria that gave much more liberal results.

Furthermore, the ASME Code approach assumes that the strain range is the expected service strain range, which is very easy to predict for a conventional pressure vessel. In contrast, the estimated strain ranges for the liner are extreme values based on conservative assumptions with a low probability of occurrence, and the expected service strain range is likely to be much less.

It is also possible that liner could be designed in accordance with the American Institute of Steel Construction (AISC) "Load and Resistance Factor Design Specification for Structural Steel Buildings" (2000). Many different types of large steel structures are designed in accord with AISC specifications, including industrial and process structures. In order to have maximum flexibility in the design and the acceptance of the design, it is recommended that, the AISC design specifications be cited in lieu of the ASME Boiler and Pressure Vessel Code if there is a choice and it is required to cite a design specification.

7.2 Available Materials

The selections of the steel plate, filler metal, and welding procedure are probably the most critical aspects of the construction documents. The requirements for the steel plate and filler metal properties are very good and are generally more stringent than what would be considered good practice in the United States. However, most of the alloys mentioned for the steel plate would be difficult to obtain in the United States. On the other hand, there are a number of good grades of steel and filler metal that are available and are described by ASTM standards. For example, steel plate and filler metal used in cold regions for gas transmission pipelines, offshore structures, ships, and even bridges provide excellent ductility and toughness. Therefore, it is recommended that the steel plate, filler metal, and weld procedure be selected after consultation with the material suppliers and qualification testing of full-scale weldments by the owner or a third party.

The requirements for the steel plate properties, including minimum Charpy requirement of 30 J at -40° C, are appropriate. As explained in Section 6.0, this requirement should provide a sufficient level of resistance to fracture. In general, when making the decision on the materials, the larger the expected Charpy value for the plate and filler metal, the better — as long as the cost premium is not too great. However, the specification of a larger "normal value" for the Charpy is meaningless in the United States and should be eliminated.

It is recommended strongly that the yield-to-tensile strength ratio be less than 0.7. This requirement is not covered in present ASTM steel specifications, but it is critically important for ductility in the plastic range. In addition, it is recommended to include maximum limits on the yield and tensile strength. These may have been implied by the referenced Swedish material standards, but this is not always covered by ASTM standards. Since the loading is strain-controlled, the strength of the plate does not have to meet any minimum standards. Because of a general inverse relation between strength and ductility and toughness, the lower the strength of the steel plate, the better. If maximum strength is limited, then hardness requirements are not needed and should not be included. Typically, hardness is not specified in the United States and could cause some problems.

There may be some changes required for the filler metal specifications. The filler metal should be required to have at least as stringent Charpy properties as the steel plate. Generally, the larger the toughness of the weld metal, the better, as defects usually are located in the welds. In bridges, for example, the Charpy requirements for the weld metal are more stringent that the requirements for the base metal.

It is also important, in order to reduce the potential for fracture, that the weld material does not yield. Therefore, there should be an explicit requirement that the strength of the filler metal overmatches the strength of the base plate. It is recommended that the ultimate strength of the filler metal is larger than the ultimate strength of the steel plate by a margin of at least 70 MPa. (The yield strength of filler normally is not specified in the United States. The overmatching requirement may have been covered by reference to the Swedish welding specifications.)

It may be impossible to find a weld filler metal with a yield-to-tensile strength ratio as low as 0.7. Because the weld metal has very low carbon content, it has an inherently high yield-to-tensile strength ratio. If the weld-metal yield strength exceeds the ultimate strength of the steel plate, the weld should never yield. Therefore, the yield-to-tensile strength ratio of the filler metal does not affect the ductility of the liner, and this requirement should be eliminated.

The chemistry requirement for the steel plate should also be eliminated. The producers should be free to provide the optimum chemistry that meets the minimum Charpy requirements and other properties. Specification of cold deformation properties is not customary in the United States and is not necessary. Weld bend tests should be required for the weld-procedure specification tests and should ensure that the steel also has adequate bend ductility.

As mentioned in Section 7.1, the issue of materials selection is related to the issue of the design specifications, because the design specifications may limit the material selections. For example, the ASME Boiler and Pressure Vessel Code allows only specific materials to be used. The AISC design specifications also has a list of approved materials. However, many of these specifications, such as ASTM A36, are very liberal and would allow whatever materials are selected to be in compliance with this specification.

7.3 Construction Practice and Welding Procedures

The requirements in the review documents for construction practice and welding procedures are very thorough. An advantage to referencing the AISC design specification is that it references the AISC "Code of Standard Practice for Steel Buildings and Bridges" included in the Manual of Steel Construction. This Code of Standard Practice includes commonly accepted standards for fabrication and erection of structural steel. The AISC specifications refer to the American Welding Society AWS D1.1 (2000), "Structural Welding Code – Steel". AWS D1.1 is widely applied as a workmanship standard for new construction of a variety of steel structures.

The welds will be 100% inspected with ultrasonic testing, and 10% randomly tested with radiographic testing. In addition, the surfaces of the welds will be inspected using either magnetic-particle or dye-penetrant techniques. These inspection requirements are sufficiently stringent, but reference should be made to AWSS D1.1 for acceptance standards.

Many of the requirements in the review documents duplicate AISC and AWS D1.1 specifications. Therefore, the construction documents should be revised to reference appropriate U.S. welding and construction codes and avoid this duplication.

8.0 CONCLUSIONS

The review presented in this report is the second phase of the review of the LRC concept. The first phase (Brandshaug et al. 2001) focused mainly on rock mechanics issues: (a) safety against uplift, and (b) effects of deformation of the rock mass on the strain range in the steel liner. The objective of the second phase (described in this report) is mainly to review the structural mechanics issues of the LRC concept. However, the main idea of the LRC concept is that the structure and the rock mass "work" together. Therefore, the rock mechanics and the structural mechanics aspects of the concept cannot be separated either during the design or in the review.

The second phase of the review considered, in more detail, the steel lining, both inside the cavern and inside the production pipe (the nozzle). The three-dimensional analyses have been conducted to investigate strains and stresses in the steel liner. In particular, the effect of discontinuities in the rock mass on strains and stresses in the steel liner was examined. (Discreteness of the rock mass was neglected by the LRC team in their analyses.) The analysis of the potential for brittle fracture and fatigue in the steel liner was reviewed. The procedures and criteria used in fracture and fatigue analysis by LRC team are considered with regard to the U.S. codes that could be applicable to potential LRC plants in the United States. Standards of construction and their compliance with the governing U.S. standards and codes were critically reviewed as well.

The analysis showed that, with regard to stresses and strains in the steel liner, both in the cavern and in the production pipe, two factors are crucial:

1. shear resistance between the steel liner and the concrete liner, and
2. the mode of deformation of the rock mass (i.e., predominantly uniform, continuous or displacement field characterized by large gradients, almost discontinuous).

The analysis showed that the strains in the steel liner are within the limits of high-cycle fatigue. However, for the most unfavorable conditions of deformation of the rock mass (jointed rock mass), and an upper bound of shear resistance in the bituminous layer between the steel and the concrete, the maximum strain is 0.31%. The allowable strain range, according to the ASME Boiler and Pressure Vessel Code, is 0.22% for 500 cycles (number of pressure cycles expected for the LRC in the United States). The analysis has shown that, in cycles following the first one, the maximum strain will decrease compared to the maximum strain in the first loading cycle. Also, the strain range is expected to be less than the maximum strain, because the residual gas pressure in the cavern will be 3 MPa. Therefore, it is expected that the strain range will be within — but very close to — the limits of the ASME Boiler and Pressure Vessel Code. The ASME limits for fillet-welded details are even more stringent: 0.15% strain range for 500 cycles. The pipe foot is fillet-welded for the cavern invert. If the rock mass is assumed to behave as continuum, the strains at the bottom of the cavern are relatively small, less than the 0.15% strain range limit. However, the analysis that assumes the discontinuous behavior of the rock mass shows that the locations of the large strain in the steel are very much controlled by the location of discontinuities in the rock mass around the

cavern. It is possible that a discontinuity that can cause relatively large steel liner strain can exist near the fillet-welded detail. Therefore, discreteness of the rock mass must be considered carefully in the analysis of the liner strains.

The effect of discontinuities in the rock mass on the steel liner strains reduces as the shear resistance in the interface between the steel and the concrete gets smaller. The analysis presented in this report for 5° friction angle in the bituminous layer overestimates the shear resistance and, therefore, is conservative. However, the analysis, as reported in Review Document 5, for a zero friction angle in the interface is certainly non-conservative and underestimates the stresses and strain in the steel liner, particularly in the production pipe (the nozzle). As a function of the shear resistance in the bituminous layer, the stresses in the production pipe in the area of transition from the cavern to the pipe exceed the allowable Tresca stress levels under certain conditions. In some cases, large compressive stresses are generated that warrant an additional buckling analysis not conducted by the LRC team (according to the review documents).

The analyses of fracture and fatigue performed in the review documents appear to be well substantiated and sufficiently conservative. However, these analyses do not address the fillet-welded details such as the pipe foot and gusset plate, shown as Detail D in drawing No. 669-025 Rev. B (Review Document 9). Preliminary estimates are that the gas storage facility should still be safe, even including the effects of the fillet-welded attachments. However, the ASME Boiler and Pressure Vessel Code would only allow a strain range of 0.15% for the fillet-welded details, which is close to the estimate of the maximum strain range. Thus, the large safety margin that was apparent in the calculations in Review Documents 1 through 3 may not be very large, and the safety of the facility may be more sensitive to the assumptions used to obtain the maximum strain range. It is recommended that the details be analyzed further using the accepted procedures in BS7910.

The review documents provide a comprehensive set of performance requirements for the overall design of the steel liner, required documentation, material requirements for steel plate and filler material, erection, welding and inspection. The technical documentation for potential LRC projects in the United States needs to be rewritten to reference appropriate U.S. codes and specifications and to avoid duplication of the provisions. It is not clear which U.S. standard should govern the design. It is our recommendation that the AISC design specifications be cited in lieu of the ASME Boiler and Pressure Vessel Code if there is a choice and if it is required to cite a design specification.

The LRC concept seems feasible from the standpoint of the structural integrity of the steel liner. However, we recommend that analysis be conducted paying more attention to details, particularly the effects of discontinuities in the rock mass and the shear resistance of the bituminous layer between the steel liner and the concrete.

9.0 REFERENCES

American Institute of Steel Construction (2000) ***Load and Resistance Factor Design Specification for Structural Steel Buildings***, Manual of Steel Construction, Third Edition. Chicago.

American Society for Testing and Materials (2001a) ***ASTM A36/A36M-01 Standard Specification for Carbon Structural Steel***.

American Society for Testing and Materials (2001b) ***ASTM A673/A673M-01 Standard Specification for Sampling Procedure for Impact testing of Structural Steel***.

American Society of Mechanical Engineers (1998a) ***ASME Boiler and Pressure Vessel Code, Section VII, Division 2, Appendix 4 — Mandatory Design Based on Stress Analysis***. New York: American Society of Mechanical Engineers.

American Society of Mechanical Engineers (1998b) ***ASME Boiler and Pressure Vessel Code, Section VIII, Division 2 — Alternative Rules***. New York: American Society of Mechanical Engineers.

American Welding Society (2000) ***Structural Welding Code – Steel***, AWS D1.1. Miami: American Welding Society.

Barsom, J. M., and S. T. Rolfe. (1987) ***Fracture and Fatigue Control in Structures***, Second Ed. Englewood Cliffs, New Jersey: Prentice-Hall.

Brandshaug, T., M. Christianson and B. Damjanac. (2001) "Technical Review of the Lined Rock Cavern (LRC) Concept and Design Methodology: Mechanical Response of Rock Mass," Technical Report ICG01-2062-1-4, Itasca Consulting Group, Inc.

British Standards Institute (1999) ***Guide on Methods for Assessing the Acceptability of Flaws in Metallic Structures***, BS 7910. London: British Standard Institute.

Itasca Consulting Group, Inc. (1998) ***3DEC (3-Dimensional Distinct Element Code)***, Version 2.0.

Itasca Consulting Group, Inc. (2002) ***FLAC3D (Fast Lagrangian Analysis of Continua in 3D)***, Version 2.1.

Larsson, H. R., R. Glamheden and G. Ahrling. (1989) "Storage of Natural Gas at High Pressure in Lined Rock Caverns — Rock Mechanics Analysis," in ***Storage of Gases in Rock Caverns***, pp. 177–184. Rotterdam: A. A. Balkema.

Paris, P., and F. Erdogan. (1962) "A Critical Analysis of Crack Propagation Laws," *Trans. ASME, Ser. D. Journal of Basic Engineering*, ***85***(4), 528–534.

Stille, H., J. Johansson and R. Sturk. (1994) "High Pressure Storage of Gas in Lined Shallow Rock Caverns — Results from Field Tests," in ***Rock Mechanics in Petroleum Engineering (Proceedings of EUROCK 94)*** , H. Roest and C. Kenter (Eds.). Rotterdam: A. A. Balkema.

Tengborg, P. (1989) "Storage of Natural Gas in Lined Rock Caverns — Studies for a Future Project in Southern Sweden," in ***Storage of Gases in Rock Caverns***, pp. 151–157. Rotterdam: A. A. Balkema.

Timoshenko, S. P., and J. N. Goodier. (1970) ***Theory of Elasticity***, Third Ed. McGraw-Hill.

U.S. Department of Energy (2000) "Advanced Gas Storage Concepts: Technology for the Future," Technical Report, National Technology Laboratory, Morgantown, West Virginia.